Weierstraß-Institut

für Angewandte Analysis und Stochastik

Leibniz-Institut im Forschungsverbund Berlin e. V.

Preprint ISSN 2198-5855

Error estimates of B-spline based finite-element method for the wind-driven ocean circulation

Nella Rotundo [1], Tae-Yeon Kim [2], Wen Jiang [3], Luca Heltai [4], Eliot Fried [5]

submitted: October 19, 2015

[1] Weierstraß-Institut
Mohrenstr. 39
10117 Berlin Germany

[2] Civil Infrastructure and Environmental Engineering
Khalifa University of Science Technology and Research
Abu Dhabi 127788 UAE

[3] Fuels Modeling and Simulation Idaho National Laboratory
Idaho Falls ID USA

[4] Scuola Internazionale Superiore di Studi Avanzati
Via Bonomea 265 34136 Trieste Italy

[5] Mathematical Soft Matter Unit Okinawa Institute of Science and Technology Graduate University
Onna Okinawa 904-0495 Japan

No. 2168

Berlin 2015

2010 *Mathematics Subject Classification.* 65M15,65D07,74S05 .

Key words and phrases. Error estimates, B-splines, geostrophisic equations, ocean circulation, Nitsche's method.

The work has been supported by (N.R.) ERC-2010-AdG no. 267802 Analysis of Multiscale Systems Driven by Functionals, and by (L.H.) project OpenViewSHIP, "Sviluppo di un ecosistema computazionale per la progettazione idrodinamica del sistema elica-carena", supported by Regione FVG - PAR FSC 2007-2013, Fondo per lo Sviluppo e la Coesione and by the project "TRIM – Tecnologia e Ricerca Industriale per la Mobilità Marina", CTN01-00176-163601, supported by MIUR, the Italian Ministry of Instruction, University and Research.

Edited by
Weierstraß-Institut für Angewandte Analysis und Stochastik (WIAS)
Leibniz-Institut im Forschungsverbund Berlin e. V.
Mohrenstraße 39
10117 Berlin
Germany

Fax: +49 30 20372-303
E-Mail: preprint@wias-berlin.de
World Wide Web: http://www.wias-berlin.de/

Abstract. We present the error analysis of a B-spline based finite-element approximation of the stream-function formulation of the large scale wind-driven ocean circulation. In particular, we derive optimal error estimates for h-refinement using a Nitsche-type variational formulations of the two simplied linear models of the stationary quasigeostrophic equations, namely the Stommel and Stommel–Munk models. Numerical results on rectangular and embedded geometries confirm the error analysis.

1. Introduction

The quasi-geostrophic equations (QGE) are one of the most widely used mathematical models for predicting the wind-driven ocean circulation at mid-latitudes (Vallis [39], Cushman-Roisin and Beckers [11], Majda [30], Majda and Wang [31], McWilliams [33], and Pedlosky [36]). Typical features of the large scale ocean flows are the formation of strong western boundary currents, weak interior flows, and weak eastern boundary currents like those exhibited by the north Atlantic and Pacific oceans. The QGE preserve these features while allowing for efficient computational simulations.

Most finite-element approximations of the QGE are based on the mixed stream-function-vorticity formulation rather than the stream-function formulation. This is because the mixed formulation is a second-order partial differential equation (PDE) that requires only low-order C^0-elements, while the stream-function formulation is a fourth-order PDE that requires higher-order C^1-elements that make implementation more challenging. To our knowledge, error estimates for the mixed formulation are suboptimal (Fix [18]). This study focuses on the stream-function formulation with optimal rates of convergence (Foster et al. [19]). Kim et al. [29] recently introduced a B-spline based finite-element discretizations of the stream-function formulations for the stationary quasi-geostrophic equations (SQGE) and two simplified linear models, namely the Stommel model and the Stommel–Munk model.

B-spline based finite-element approximations offer two distinct advantages over standard Lagrangian based finite-element methods: a) high order continuity can be obtained at a relatively low computational cost, and b) curved and complex geometries can be represented exactly using B-splines and NURBS basis functions (see, for example Hughes et al. [22]). Their versatility makes these approximation spaces ideal also in conjunction with other techniques, such as boundary element methods (Heltai et al. [21]) or reduced basis methods (Manzoni et al. [32]). On the other hand, since, B-spline spaces are non-interpolatory, and imposing even simple boundary conditions can be problematic. Additionally, for problems where the formation of boundary layers is important, the imposition of boundary conditions in a strong manner may not be appropriate, since doing so may induce artificial oscillations and may also reduce the accuracy of whatever underlying numerical method is employed (see, for example, Bazilevs and Hughes [2]).

Kim et al. [29] developed variational formulations for the stream-function formulation of the SGQE, the Stommel model, and the Stommel–Munk model which are

Date: October 21, 2015.

also valid for non-interpolatory basis functions such as B-splines, and which also work well for embedded geometries, where the domain may be implicitly defined via a level-set function. In these formulations the Drichlet boundary conditions are weakly enforced and stabilization is achieved via Nitsche's method (Nitsche [35]). Recently, Nitsche's method has been successfully applied to weakly impose boundary and interfacial conditions for the second- and fourth-order PDE (Embar et al. [15], Kim et al. [26], Kim and Dolbow [25], Kim et al. [27], and Kim et al. [28]) and meshfree (Fernández-Méndez and Huerta [17]) and embedded finite-element methods (Hansbo and Hansbo [20] and Dolbow and Harari [13]). The use of Nitsche's method [35] to impose boundary conditions on complex geometries also generalises very easily to embedded finite-element methods, including the immersogeometric approach of Kamensky et al. [24] and the formulation of Nitsche's method due to Jiang et al. [23]. Such methods can be seen as a B-spline generalisation of immersed finite-element methods (see, for example, Boffi et al. [5] and the references therein).

The main goal of this paper is to derive optimal error estimates for h-refinement of the Nitsche-type finite-element formulations introduced by Kim et al. [29] for the Stommel and Stommel–Munk models. We also provide convergence results through several benchmark problems both on rectangular geometries as well as on embedded geometries and verify these error estimates using cubic B-splines approximations.

The remainder of the paper is organized as follows. In Section 2 we briefly recount the features of B-spline based finite dimensional spaces and their approximation properties most relevant to our considerations. Sections 3 and 4 are respectively devoted to the optimal error estimates for the Nitsche-type variational formulations of the Stommel model and the Stommel–Munk model. In Section 5, we present two examples which demonstrate that the analysis in Section 3 and 4 is optimal in both rectangular and embedded domains. Finally, conclusions and a brief discussion of potential future research directions are contained in Section 6.

2. B-spline spaces

Conforming finite-element approximations of boundary value problems for fourth-order partial differential equations, such as the Stommel–Munk model, require the construction of globally C^1-continuous basis functions. A popular choice of a finite dimensional space which satisfies such constraints is the finite-element space based on tensor products between cubic B-splines that are globally C^2-continuous and strike a good balance between approximation properties, computational costs, and implementational issues.

A general scalar function v_h in a one-dimensional B-spline approximation space can be written as

$$v_h(s) = \sum_{i=1}^{n} N_{i,p}(s) v_i, \qquad s \in [0,1], \tag{2.1}$$

where v_i is usually referred to as the i-th control value. Here, $N_{i,p}$ is the i-th B-spline basis function of degree p and s denotes a parametric coordinate. B-spline curves in two and three dimensions are obtained by replacing the control values v_i with control points P_i in two or three dimensions.

A brief account of the B-spline basis functions in one dimension is given below. Consider a non-decreasing set of real values k_i, also known as knot vector k, where

$$k = \{0 = k_1 \leq k_2 \leq \ldots \leq k_{n+p+1} = 1\}, \tag{2.2}$$

with n denoting the number of basis functions and p the degree of the spline. B-spline basis functions are defined recursively starting with piecewise constants

(degree $p = 0$):

$$N_{i,0}(s) = \begin{cases} 1 & \text{if } k_i \leq s < k_{i+1}, \\ 0 & \text{otherwise.} \end{cases} \tag{2.3}$$

For $p \geq 1$,

$$N_{i,p}(s) = \frac{s - k_i}{k_{i+p} - k_i} N_{i,p-1}(s) + \frac{k_{i+p+1} - s}{k_{i+p+1} - k_{i+1}} N_{i+1,p-1}(s), \tag{2.4}$$

where the knot-dependent factors are replaced with zero when the denominator vanishes. If the first and last knots are repeated $p + 1$ times, then the knot vector is said to be *open*, and it is interpolatory at its extremes. If no internal knots are repeated, then the resulting B-spline basis functions are globally C^{p-1} continuous. For simplicity, we will restrict attention to situations where all knot vectors are open, with no internal repetitions.

Extension to multiple dimensions is straightforward with the use of tensor product splines. (For a more detailed treatment of the subject see Piegl and Tiller [37] or Cottrell et al. [10].) In particular we construct two-dimensional B-splines by taking the tensor product of B-splines with the same order in each coordinate direction.

We consider a Lipschitz open set $\Omega \in \mathbb{R}^2$, with boundary $\partial\Omega = \Gamma$, and for simplicity we assume that such geometrical domain can be represented exactly by an invertible B-spline map $F : Q := [0,1] \times [0,1] \to \bar{\Omega}$, defined through the geometrical control points $\mathbf{P}_i$ in accord with

$$F(\mathbf{s}) = \sum_{i=1}^{n} \mathbf{N}_{i,p}(\mathbf{s}) \mathbf{P}_i = \mathbf{x} \in \Omega \subset \mathbb{R}^2, \qquad \mathbf{s} \in Q := [0,1] \times [0,1], \tag{2.5}$$

where we denote with $\mathbf{N}_{i,p}$ the two-dimensional i-th B-spline of degree p obtained through the tensor product of two one-dimensional B-splines of order p.

We assume that the control points $\mathbf{P}_i$ are such that the geometrical map F satisfies the following property for $p \geq 1$, so that

$$|v \circ F|_{H^p_Q} \leq C \|v\|_{H^p_\Omega}, \forall v \in H^p(\Omega), \qquad |u \circ F^{-1}|_{H^p_\Omega} \leq C \|u\|_{H^p_Q}, \forall u \in H^p(Q), \tag{2.6}$$

where $C = C(F, p)$, and $|\cdot|_{H^p_Q}$ (resp. $\|\cdot\|_{H^p_Q}$) indicate the standard Sobolev seminorm (resp. norm) in the space $H^p(Q)$, and the symbol $\circ$ indicates the composition of functions.

More complex geometrical representations are of course possible, provided that they stitch together with the correct continuity and that a property similar to equation (2.6) is kept. (See Cottrell et al. [10] for an in depth treatment on the subject of multi-patch geometries, and da Veiga et al. [12] for more details on the requirements of the geometrical map.)

In this work we assume a single patch geometry for simplicity, and we provide a rigorous analysis for the case where the geometry is defined as in (2.5); however, our results are easily extendible to multipatch geometries and to situations where the shape of the boundary is defined implicitly using a level-set function, as in the work of Jiang et al. [23]. The convergence properties of the resulting method depend on the embedding space, and some evidence indicating that the analysis carries over also to these cases is provided in Section 5.

The geometrical representation presented in equation (2.5) defines naturally a space of finite dimension n as the span of the basis functions $\tau_{i,p}$ implicitly determined through the push-forward of the B-spline basis functions through F:

$$\tau_{i,p}(F(\mathbf{s})) := \mathbf{N}_{i,p}(\mathbf{s}), \qquad \mathbf{s} \in Q := [0,1] \times [0,1], \qquad i = 1, \ldots, n. \tag{2.7}$$

The geometrical map F induces naturally a partition of the domain Ω, $\mathcal{P}(\Omega) = \{\Omega_e\}_{e=1}^{N_{\text{el}}}$, into N_{el} number of elements Ω_e, given by the image through F of the tensor product of two consecutive, non-repeated, knot points in each of the coordinate directions of $\mathbf{s}$. We define $h_e = \text{diam}(\Omega_e)$ as the element characteristic dimension and $h := \max_{\Omega_e \in \mathcal{P}(\Omega)} h_e$ as the *global mesh parameter*. We also define $\Gamma_e = \partial\Omega_e \cap \Gamma$, $\forall \Omega_e \in \mathcal{P}(\Omega)$, where $\partial\Omega_e$ is the boundary of each element of the partition.

For any element $\Omega_e \in \mathcal{P}(\Omega)$, the pull-back of τ_i through the map F is a polynomial of order p in each coordinate direction.

The space $\mathcal{Q}_h^p$ defined by

$$\mathcal{Q}_h^p := \text{span}\left\{\tau_{i,p} := \mathbf{N}_{i,p} \circ F^{-1}\right\}_{i=1}^{n} \subset C^{p-1}(\overline{\Omega}) \subset H^p(\Omega), \tag{2.8}$$

is globally C^{p-1}-continuous and $H^p(\Omega)$ conforming.

For each space $\mathcal{Q}_h^p$ it is possible to construct a B-spline preserving operator $\mathcal{I}_h^p : H^p(\Omega) \to \mathcal{Q}_h^p$ such that the estimate (see Bazilevs et al. [3] and da Veiga et al. [12])

$$\begin{aligned} &\mathcal{I}_h^p q = q \qquad \forall q \in \mathcal{Q}_h^p, \\ &|u - \mathcal{I}_h^p u|_{H_\Omega^m} \leq C h^{k+1-m} |u|_{H_\Omega^{k+1}}, \quad \forall u \in H^{k+1}(\Omega), \qquad 0 \leq m < k \leq p, \end{aligned} \tag{2.9}$$

holds, where C depends on F and p, but not on h. A stronger result is easily obtained by considering the full norms:

$$\|u - \mathcal{I}_h^p u\|_{H_\Omega^m} \leq C h^{k+1-m} \|u\|_{H_\Omega^{k+1}}, \quad \forall u \in H^{k+1}(\Omega), \qquad 0 \leq m < k \leq p. \tag{2.10}$$

We recall now some well known and useful inequalities and definitions than can be found for example in Ciarlet [9], Brenner and Scott [7] and Engel et al. [16] (for general finite-element techniques), and in Bazilevs et al. [3] and da Veiga et al. [12] (for B-spline based finite-element approximations).

2.1. **Inverse estimates.**

Theorem 2.1. *Let $\mathcal{Q}_h^p$ be one of the finite dimensional spaces defined in* (2.8) *and let l and m be two positive integers satisfying*

$$l \leq m.$$

Then there exists a constant C depending only on F, p, and l such that

$$|u|_{H_{\Omega_e}^m} \leq C h_e^{l-m} |u|_{H_{\Omega_e}^l}, \qquad \forall u \in \mathcal{Q}_h^p. \tag{2.11}$$

The above estimate implies the stronger result

$$\|u\|_{H_{\Omega_e}^m} \leq C h_e^{l-m} \|u\|_{H_{\Omega_e}^l}, \qquad \forall u \mathcal{Q}_h^p. \tag{2.12}$$

2.2. **Trace of Sobolev space functions.**

Theorem 2.2. *Arnold [1], Ciarlet [9]: Let $\Omega_e \subset \mathbb{R}^d$ with Lipschitz boundary Γ_e. Then there exists a constant C such that*

$$\|u\|_{L_{\Gamma_e}^2}^2 \leq C(h_e^{-1} \|u\|_{L_{\Omega_e}^2}^2 + h_e \|\nabla u\|_{L_{\Omega_e}^2}^2), \qquad \forall u \in H_{\Omega_e}^1. \tag{2.13}$$

One of the consequence of the trace inequality is that if $u \in \mathcal{Q}_h^p$ we can combine (2.13) and (2.11) with $l = 0$ and $m = 1$, and obtain

$$\begin{aligned} \|u\|_{L_{\Gamma_e}^2}^2 &\leq C_1(h_e^{-1} \|u\|_{L_{\Omega_e}^2}^2 + h_e |u|_{H_{\Omega_e}^1}^2) \\ &\leq C_2(h_e^{-1} \|u\|_{L_{\Omega_e}^2}^2 + h_e h_e^{-2} |u|_{H_{\Omega_e}^0}^2) \\ &= C_2(h_e^{-1} \|u\|_{L_{\Omega_e}^2}^2 + h_e^{-1} \|u\|_{L_{\Omega_e}^2}^2) \\ &\leq C_3 h_e^{-1} \|u\|_{L_{\Omega_e}^2}^2 \qquad \forall u \in \mathcal{Q}_h^p. \end{aligned} \tag{2.14}$$

Theorem 2.3. *Let $\Omega_e \subset \mathbb{R}^d$ a Lipschitz domain and $1/2 < s \leq 1$. Then there exists a unique linear bounded trace mapping*

$$\begin{aligned} \gamma_0 : H^s_{\Omega_e} &\to H^{s-1/2}_{\Gamma_e} \\ u &\longmapsto \gamma_0(u) := u_{|\Gamma_e} \end{aligned}$$

such that

$$\begin{aligned} \|\gamma_0(u)\|_{H^{s-1/2}_{\Gamma_e}} &\leq C_T \|u\|_{H^s_{\Omega_e}}, \\ |\gamma_0(u)|_{H^{s-1/2}_{\Gamma_e}} &\leq C_T |u|_{H^s_{\Omega_e}}. \end{aligned}$$

Moreover this trace operator has a bounded right inverse

$$\gamma_0^- : H^{s-1/2}_{\Gamma_e} \to H^s_{\Omega_e};$$

that is $\gamma_0 \gamma_0^- u = u$, $u \in H^{s-1/2}_{\Gamma_e}$, and

$$\begin{aligned} \|\gamma_0^-(u)\|_{H^s_{\Omega_e}} &\leq C_T \|u\|_{H^{s-1/2}_{\Gamma_e}}, \\ |\gamma_0^-(u)|_{H^s_{\Omega_e}} &\leq C_T |u|_{H^{s-1/2}_{\Gamma_e}}. \end{aligned}$$

In the following sections we will concentrate on B-spline finite dimensional spaces which are either H^1-conforming (for the Stommel model) or H^2-conforming (for the Stommel-Munk model). For ease of notation, we use $\mathcal{V}^h$ to indicate the family of spaces which are H^1-conforming, i.e.,

$$\mathcal{V}_h := \mathcal{Q}_h^p \quad p \geq 1; \tag{2.15}$$

further, we use $\mathcal{W}^h$ to indicate the family of H^2-conforming finite-element spaces, i.e.,

$$\mathcal{W}_h := \mathcal{Q}_h^p \quad p \geq 2. \tag{2.16}$$

We will drop the indication on the degree p and the mesh size h from the operator $\mathcal{I}_h^p$, and thus simply use $\mathcal{I}$ to indicate either an operator for $\mathcal{V}_h$ or $\mathcal{W}_h$ depending on context.

3. The Stommel Model

3.1. **Variational formulation of the Stommel Model.** We consider a Lipschitz open set $\Omega \in \mathbb{R}^2$, with boundary $\partial\Omega = \Gamma$, and use the notation $\mathbf{x} = (x, y) \in \Omega$. The Stommel model is given by

$$\begin{aligned} -\epsilon_{\mathrm{s}} \Delta \psi - \frac{\partial \psi}{\partial x} &= F \quad \text{in } \Omega, \\ \psi &= 0 \quad \text{on } \Gamma, \end{aligned} \tag{3.1}$$

where ϵ_{s} is the Stommel number

$$\epsilon_{\mathrm{s}} = \frac{\gamma}{\beta L},$$

with γ being the coefficient of the linear drag (or the Rayleigh friction), as might be generated by a bottom Ekman layer, L is the characteristic length scale, and β is the coefficient multiplying the y-coordinate in the β-plane approximation (Cushman-Roisin and Beckers [11] or Vallis [39, Section 2.3.2]).

We introduce the Hilbert space

$$\mathcal{V} := H^1_0(\Omega) = \left\{ \phi \in H^1(\Omega) : \phi = 0 \quad \text{on } \Gamma \right\}, \tag{3.2}$$

where $H^1(\Omega)$ is the standard Sobolev space of square-integrable functions with square-integrable first derivatives in Ω. Multiplying $(3.1)_1$ by a test function $\phi \in \mathcal{V}$, integrating by parts over Ω and taking into account the boundary conditions, one

obtains the classical variational formulation of the Stommel model, which can be expressed as: find $\psi \in \mathcal{V}$ such that

$$a(\psi, \phi) = \ell(\phi), \qquad \forall\, \phi \in \mathcal{V}, \tag{3.3}$$

where a is a bilinear form $a(\cdot,\cdot) : \mathcal{V} \times \mathcal{V} \to \mathbb{R}$ defined by

$$a(\psi, \phi) := \int_\Omega \epsilon_{\mathrm{s}} \nabla\psi \cdot \nabla\phi \,\mathrm{d}\Omega - \int_\Omega \frac{\partial \psi}{\partial x}\phi \,\mathrm{d}\Omega \qquad \forall \psi, \phi \in \mathcal{V}, \tag{3.4}$$

and

$$\ell(\phi) := \int_\Omega F\phi \,\mathrm{d}\Omega, \qquad \forall \phi \in \mathcal{V}. \tag{3.5}$$

3.2. **Nitsche's formulation of the Stommel model.** The standard variational formulation (3.3) can be used as is for conforming approximations, with boundary conditions being enforced strongly in the space $\mathcal{V}_h$.

Although B-spline basis functions are non-interpolatory, they can be made to enforce strongly the boundary conditions in $(3.1)_2$. This has been shown to have drawbacks for the numerical simulation of flow problems where boundary layer effects may be important. This is the case for turbulent flows (Bazilevs and Hughes [2] and Bazilevs et al. [4]) and it plays an important role also for QGE models.

The weak formulation of the QGE models we analyse here was introduced in Kim et al. [29] and represents a viable and robust alternative to the strong imposition of boundary conditions. The use of a weak formulation to impose Dirichlet boundary conditions was first introduced in Nitsche [35]. Such techniques have been shown to yield optimal rates of convergence for h-refinement in finite-element approximations (Embar et al. [15]).

As is standard in these cases, we proceed by considering the sum

$$\widetilde{\mathcal{V}} = \mathcal{V} + \mathcal{V}_h,$$

of the spaces $\mathcal{V}$ and $\mathcal{V}_h$, where $\mathcal{V}_h$ is defined in (2.15). In the following, Greek letters denote functions belonging to $\mathcal{V}$, Greek letters subscribed with h deonte functions belonging to $\mathcal{V}_h$, and Greek letters with superposed tildes denote functions belonging to $\widetilde{\mathcal{V}}$.

We approximate (3.3) by the finite dimensional variational problem: find $\psi_h \in \mathcal{V}_h$ such that

$$a_h(\psi_h, \phi_h) = \ell(\phi_h), \qquad \forall\, \phi_h \in \mathcal{V}_h, \tag{3.6}$$

where the approximate bilinear form $a_h(\cdot,\cdot) : \widetilde{\mathcal{V}} \times \widetilde{\mathcal{V}} \to \mathbb{R}$ is defined by

$$\begin{aligned} a_h(\widetilde{\psi}, \widetilde{\phi}) = &\int_\Omega \epsilon_{\mathrm{s}} \nabla\widetilde{\psi} \cdot \nabla\widetilde{\phi} \,\mathrm{d}\Omega - \int_\Omega \frac{\partial \widetilde{\psi}}{\partial x}\widetilde{\phi} \,\mathrm{d}\Omega \\ &- \int_\Gamma \epsilon_{\mathrm{s}} (\nabla\widetilde{\psi} \cdot \mathbf{n})\widetilde{\phi} \,\mathrm{d}\Gamma - \int_\Gamma \epsilon_{\mathrm{s}} (\nabla\widetilde{\phi} \cdot \mathbf{n})\widetilde{\psi} \,\mathrm{d}\Gamma + \alpha \int_\Gamma \widetilde{\phi}\widetilde{\psi} \,\mathrm{d}\Gamma, \end{aligned} \tag{3.7}$$

where $\mathbf{n}$ is the unit outward normal vector.

The second-line contains a penalisation term which is used to weakly impose the boundary condition $(3.1)_2$, depending on the stabilisation parameter α, and two terms which ensure consistency of the bilinear form. Notice that if we choose ψ and χ belonging to $\mathcal{V}$, the bilinear form a_h in (3.7) coincides with a in (3.4), i.e., the second-line is identically zero because $\psi = \chi = 0$ on Γ. The bilinear form a_h in (3.7) suggests the introduction of the following stabilization dependent norm in $\widetilde{\mathcal{V}}$ (see, for example, Engel et al. [16])

$$|||\widetilde{\psi}|||_1^2 := \|\epsilon_s^{1/2}\nabla\widetilde{\psi}\|_{L^2_\Omega}^2 + \|\alpha^{1/2}\widetilde{\psi}\|_{L^2_\Gamma}^2. \tag{3.8}$$

For later use, we introduce the following remark and lemma:

Remark 3.1 (Strong consistency)**.** *If we multiply* $(3.1)_1$ *by a test function* $\phi_h \in \mathcal{V}_h$*, integrate by parts and take into account the boundary condition on* $\psi \in \mathcal{V}$*, we see that*

$$\int_\Omega \epsilon_s \nabla\psi\cdot\nabla\phi_h \, d\Omega - \int_\Gamma \epsilon_s(\nabla\psi\cdot\mathbf{n})\phi_h \, d\Gamma - \int_\Omega \frac{\partial\psi}{\partial x}\phi_h \, d\Omega = \int_\Omega F\phi_h \, d\Omega,$$

which is, from (3.7) *and* (3.5)*,*

$$a_h(\psi,\phi_h) - \ell(\phi_h) = 0, \qquad \forall\phi_h \in \mathcal{V}_h.$$

Notice that the last two terms on the second line in (3.7) *vanish since* ψ *satisfies the boundary condition* $\psi = 0$ *on* Γ*.*

Lemma 3.1. *There is a positive constant* c_I *such that (Bramble et al. [6])*

$$\sum_{\Gamma_e} h_e \left\| \frac{\partial\phi_h}{\partial\mathbf{n}} \right\|^2_{L^2_{\Gamma_e}} \le c_I \|\nabla\phi_h\|^2_{L^2_\Omega}, \quad \forall\phi_h \in \mathcal{V}_h.$$

Thanks to the lemma 3.1, we can write the following inverse estimate

$$\|\nabla\psi_h\cdot\mathbf{n}\|^2_{L^2_\Gamma} \le Ch^{-1}\|\nabla\psi_h\|^2_{L^2_\Omega}, \quad \forall\psi_h \in \mathcal{V}_h, \tag{3.9}$$

for a positive constant C.

3.3. Ellipticity and continuity of the bilinear form a_h.

Proposition 3.1. *It is possible to choose the stabilization parameter* α *such that the bilinear form* (3.7) *is uniformly* $\mathcal{V}_h$*-elliptic; i.e., there exists a constant* $M > 0$ *such that*

$$a_h(\psi_h,\psi_h) \ge M|||\psi_h|||_1^2, \quad \forall\psi_h \in \mathcal{V}_h \tag{3.10}$$

where M *is independent of both* h *and* α*.*

Proof. Replacing both $\widetilde{\psi}$ and $\widetilde{\phi}$ by ψ_h in (3.7) yields

(3.11)

$$a_h(\psi_h,\psi_h) = \|\epsilon_s^{1/2}\nabla\psi_h\|^2_{L^2_\Omega} + \|\alpha^{1/2}\psi_h\|^2_{L^2_\Gamma} - 2\int_\Gamma \epsilon_s(\nabla\psi_h\cdot\mathbf{n})\psi_h \, d\Gamma - \int_\Omega \frac{\partial\psi_h}{\partial x}\psi_h \, d\Omega.$$

We recall the following Young's inequality on a Lipschitz domain $E \in \mathbb{R}^d$, with $d = 1, 2$ or 3

$$\int_E fg \, d\Omega \le \frac{\delta}{2}\|f\|^2_{L^2(E)} + \frac{1}{2\delta}\|g\|^2_{L^2(E)}, \tag{3.12}$$

for any arbitrary constant $\delta > 0$. Using (3.9) and (3.12), the third term on the right-hand side of (3.11) admits the estimate

$$\begin{aligned} -2\int_\Gamma \epsilon_s(\nabla\psi_h\cdot\mathbf{n})\psi_h \, d\Gamma &\ge -\delta\|\epsilon_s(\nabla\psi_h\cdot\mathbf{n})\|^2_{L^2_\Gamma} - \frac{1}{\delta}\|\psi_h\|^2_{L^2_\Gamma} \\ &\ge -\delta\epsilon_s Ch^{-1}\|\epsilon_s^{1/2}\nabla\psi_h\|^2_{L^2_\Omega} - \frac{1}{\delta\alpha}\|\alpha^{1/2}\psi_h\|^2_{L^2_\Gamma}. \end{aligned} \tag{3.13}$$

We can rewrite the last integral in (3.11) as

$$\int_\Omega \frac{\partial\psi_h}{\partial x}\psi_h \, d\Omega = \int_\Omega (\nabla\psi_h\cdot\mathbf{e}_x)\psi_h \, d\Omega = \int_\Omega \nabla\psi_h\cdot(\psi_h\mathbf{e}_x) \, d\Omega, \tag{3.14}$$

where $\mathbf{e}_x = (1,0)$ is the base vector along the x-direction. Applying the divergence theorem to (3.14) yields

$$\begin{aligned}\int_\Omega \nabla\psi_h \cdot (\psi_h \mathbf{e}_x)\,\mathrm{d}\Omega &= \int_\Gamma (\psi_h)^2 \mathbf{n}\cdot\mathbf{e}_x\,\mathrm{d}\Gamma - \int_\Omega \psi_h \nabla\cdot(\psi_h\mathbf{e}_x)\,\mathrm{d}\Omega \\ &= \int_\Gamma (\psi_h)^2 \mathbf{n}\cdot\mathbf{e}_x\,\mathrm{d}\Gamma - \int_\Omega \nabla\psi_h\cdot(\psi_h\mathbf{e}_x)\,\mathrm{d}\Omega,\end{aligned}$$

where $\mathbf{n}$ is the unit outward normal vector. Finally, we obtain the inequality

$$\int_\Omega \frac{\partial\psi_h}{\partial x}\psi_h\,\mathrm{d}\Omega = \frac{1}{2}\int_\Gamma (\psi_h)^2\mathbf{n}\cdot\mathbf{e}_x\,\mathrm{d}\Gamma \le \frac{1}{2}\|\psi_h\|^2_{L^2_\Gamma}. \tag{3.15}$$

Applying the inequalities (3.13) and (3.15) to (3.11) results in

$$\begin{aligned}a_h(\psi_h,\psi_h) &\ge \left(1-\delta\epsilon_{\mathrm{s}}Ch^{-1}\right)\|\epsilon_{\mathrm{s}}^{1/2}\nabla\psi_h\|^2_{L^2_\Omega} + \left(1-\frac{1}{\delta\alpha}-\frac{1}{2\alpha}\right)\|\alpha^{1/2}\psi_h\|^2_{L^2_\Gamma} \\ &\ge M|||\psi_h|||_1^2.\end{aligned}$$

Since M must be a positive constant, we choose δ and α such that the terms $(1-\delta\epsilon_{\mathrm{s}}Ch^{-1})$ and $(1-1/(\delta\alpha)-1/(2\alpha))$ are equal (to M). We find that the first term is granted positive if $\delta < h/(\epsilon_{\mathrm{s}}C)$. Taking $\delta = ph/(\epsilon_{\mathrm{s}}C)$ with any $p\in(0,1)$ yields

$$\alpha = \frac{1}{2p} + \frac{\epsilon_{\mathrm{s}}C}{p^2}h^{-1} \tag{3.16}$$

and the constant M is positive and it is equal to $1-p$, independent of the values of both h and α. □

Let h_0 such that $\frac{\epsilon_{\mathrm{s}}C}{(1-p)^2}h_0^{-1} >> \frac{1}{2(1-p)}$, then, for $h < h_0$, (3.16) suggests that

$$\alpha \sim \frac{1}{h}. \tag{3.17}$$

Lemma 3.2. *For all $\widetilde{\psi}\in\widetilde{\mathcal{V}}$ the following inequality holds*

$$\|\widetilde{\psi}\|^2_{L^2_\Omega} \le c|||\widetilde{\psi}|||_1 \tag{3.18}$$

for some positive constant c. Moreover, on choosing α as dictated by (3.16)*, we conclude that the constant c is independent of h.*

Proof. Since $\widetilde{\psi}\in\widetilde{\mathcal{V}}$ we have $\|\widetilde{\psi}\|^2_{L^2_\Omega} = \|\psi+\psi_h\|^2_{L^2_\Omega}$. Thus, by the Poincaré inequality

$$\|\widetilde{\psi}\|^2_{L^2_\Omega} \le \|\psi\|^2_{L^2_\Omega} + \|\psi_h\|^2_{L^2_\Omega} \le C_P|\psi|^2_{H^1_\Omega} + \|\psi_h\|^2_{L^2_\Omega}.$$

Summing and subtracting in the first term the quantity ψ_h we can write

$$\begin{aligned}\|\widetilde{\psi}\|^2_{L^2_\Omega} &\le C_P|\widetilde{\psi}|^2_{H^1_\Omega} + C_P|\psi_h|^2_{H^1_\Omega} + \|\psi_h\|^2_{L^2_\Omega} \\ &\le \frac{C_P}{\epsilon_{\mathrm{s}}}\|\epsilon_{\mathrm{s}}^{1/2}\nabla\widetilde{\psi}\|^2_{L^2_\Omega} + C_P|\psi_h|^2_{H^1_\Omega} + \|\psi_h\|^2_{L^2_\Omega} \\ &\le \frac{C_P}{\epsilon_{\mathrm{s}}}\|\epsilon_{\mathrm{s}}^{1/2}\nabla\widetilde{\psi}\|^2_{L^2_\Omega} + C_2\|\psi_h\|^2_{H^1_\Omega},\end{aligned}$$

with $C_2 = \max\{C_P, 1\}$. Using the trace inequality (see Theorem 2.3) we arrive at the inequality

$$\begin{aligned}\|\widetilde{\psi}\|^2_{L^2_\Omega} &\le \frac{C_P}{\epsilon_{\mathrm{s}}}\|\epsilon_{\mathrm{s}}^{1/2}\nabla\widetilde{\psi}\|^2_{L^2_\Omega} + C_T\|\psi_h\|^2_{H^{1/2}_\Gamma} \\ &\le \frac{C_P}{\epsilon_{\mathrm{s}}}\|\epsilon_{\mathrm{s}}^{1/2}\nabla\widetilde{\psi}\|^2_{L^2_\Omega} + \frac{C_3}{h\alpha}\|\alpha^{1/2}\psi_h\|^2_{L^2_\Gamma}.\end{aligned}$$

In the last inequality we have we have applied (2.12) on the grounds that $\psi_h \in \mathcal{V}_h$. Finally, since $\psi \in \mathcal{V} \subset H_0^1(\Omega)$ vanishes on the boundary, we deduce the estimate

$$\|\widetilde{\psi}\|_{L^2_\Omega}^2 \leq \frac{C_P}{\epsilon_{\mathrm{s}}}\|\epsilon_{\mathrm{s}}^{1/2}\nabla\widetilde{\psi}\|_{L^2_\Omega}^2 + \frac{C_3}{h\alpha}\|\alpha^{1/2}\widetilde{\psi}\|_{L^2_\Gamma}^2. \tag{3.19}$$

On taking $c = \max\left\{\frac{C_P}{\epsilon_{\mathrm{s}}}, \frac{C_3}{h\alpha}\right\}$ and considering the definition (3.8) of the norm $|||\cdot|||_1$, (3.19) leads to (3.18), with c independent of h as long as α is chosen as in (3.16). □

Proposition 3.2. *If we choose the stabilization parameter as in equation (3.16), then the bilinear form* (3.7) *is uniformly continuous in $\widetilde{\mathcal{V}}$ with respect to the norm $|||\cdot|||_1$, i.e.,*

$$|a_h(\widetilde{\psi},\widetilde{\chi})| \leq c|||\widetilde{\psi}|||_1\ |||\widetilde{\chi}|||_1 \qquad \forall\widetilde{\psi},\widetilde{\chi}\in\widetilde{\mathcal{V}},$$

with c independent of both h and α.

Proof. Using Hölder's inequality in (3.7), we have

$$\begin{aligned}\left|a_h(\widetilde{\psi},\widetilde{\phi})\right| \leq& \|\epsilon_{\mathrm{s}}^{1/2}\nabla\widetilde{\psi}\|_{L^2_\Omega}\|\epsilon_{\mathrm{s}}^{1/2}\nabla\widetilde{\phi}\|_{L^2_\Omega} + \|\alpha^{1/2}\widetilde{\psi}\|_{L^2_\Gamma}\|\alpha^{1/2}\widetilde{\phi}\|_{L^2_\Gamma}\\ &+ \frac{\epsilon_{\mathrm{s}}^{1/2}}{\alpha^{1/2}}\|\epsilon_{\mathrm{s}}^{1/2}\nabla\widetilde{\psi}\cdot\mathbf{n}\|_{L^2_\Gamma}\|\alpha^{1/2}\widetilde{\phi}\|_{L^2_\Gamma} + \frac{\epsilon_{\mathrm{s}}^{1/2}}{\alpha^{1/2}}\|\epsilon_{\mathrm{s}}^{1/2}\nabla\widetilde{\phi}\|_{L^2_\Gamma}\|\alpha^{1/2}\widetilde{\psi}\|_{L^2_\Gamma}\\ &+ \int_\Omega\left|\frac{\partial\widetilde{\psi}}{\partial x}\widetilde{\phi}\right|\,\mathrm{d}\Omega.\end{aligned} \tag{3.20}$$

The last term can be estimated using Lemma 3.2:

$$\int_\Omega\left|\frac{\partial\widetilde{\psi}}{\partial x}\widetilde{\phi}\right|\,\mathrm{d}\Omega \leq \|\nabla\widetilde{\psi}\|_{L^2_\Omega}\|\widetilde{\phi}\|_{L^2_\Omega} \leq \frac{C}{\epsilon_{\mathrm{s}}^{1/2}}\|\epsilon_{\mathrm{s}}^{1/2}\nabla\widetilde{\psi}\|_{L^2_\Omega}|||\widetilde{\phi}|||_1. \tag{3.21}$$

Applying (3.9), (3.21), and Hölder's inequality to (3.20) results in

$$\begin{aligned}|a_h(\widetilde{\psi},\widetilde{\phi})| \leq& \|\epsilon_{\mathrm{s}}^{1/2}\nabla\widetilde{\psi}\|_{L^2_\Omega}\|\epsilon_{\mathrm{s}}^{1/2}\nabla\widetilde{\phi}\|_{L^2_\Omega} + \|\alpha^{1/2}\widetilde{\psi}\|_{L^2_\Gamma}\|\alpha^{1/2}\widetilde{\phi}\|_{L^2_\Gamma}\\ &+ \frac{(\epsilon_{\mathrm{s}}C)^{1/2}}{(\alpha h)^{1/2}}\|\epsilon_{\mathrm{s}}^{1/2}\nabla\widetilde{\psi}\|_{L^2_\Omega}\|\alpha^{1/2}\widetilde{\phi}\|_{L^2_\Gamma} + \frac{(\epsilon_{\mathrm{s}}C)^{1/2}}{(\alpha h)^{1/2}}\|\epsilon_{\mathrm{s}}^{1/2}\nabla\widetilde{\phi}\|_{L^2_\Omega}\|\alpha^{1/2}\widetilde{\psi}\|_{L^2_\Gamma}\\ &+ \frac{C}{\epsilon_{\mathrm{s}}}\|\epsilon_{\mathrm{s}}^{1/2}\nabla\widetilde{\psi}\|_{L^2_\Omega}|||\widetilde{\phi}|||_1\\ =&\|\epsilon_{\mathrm{s}}^{1/2}\nabla\widetilde{\psi}\|_{L^2_\Omega}\left(\|\epsilon_{\mathrm{s}}^{1/2}\nabla\widetilde{\phi}\|_{L^2_\Omega} + \frac{C}{\epsilon_{\mathrm{s}}^{1/2}}|||\widetilde{\phi}|||_1\right)\\ &+ \frac{(\epsilon_{\mathrm{s}}C)^{1/2}}{(h\alpha)^{1/2}}\left(\|\epsilon_{\mathrm{s}}^{1/2}\nabla\widetilde{\psi}\|_{L^2_\Omega}\|\alpha^{1/2}\widetilde{\phi}\|_{L^2_\Gamma} + \|\epsilon_{\mathrm{s}}^{1/2}\nabla\widetilde{\phi}\|_{L^2_\Omega}\|\alpha^{1/2}\widetilde{\psi}\|_{L^2_\Gamma}\right)\\ \leq& c\left(\|\epsilon_{\mathrm{s}}^{1/2}\nabla\widetilde{\psi}\|_{L^2_\Omega} + \|\alpha^{1/2}\widetilde{\psi}\|_{L^2_\Gamma}\right)\left(\|\epsilon_{\mathrm{s}}^{1/2}\nabla\widetilde{\phi}\|_{L^2_\Omega} + \|\alpha^{1/2}\widetilde{\phi}\|_{L^2_\Gamma}\right)\\ \leq& c|||\widetilde{\psi}|||_1\ |||\widetilde{\phi}|||_1,\end{aligned}$$

where

$$c = \max\left\{1 + \frac{C}{\epsilon_{\mathrm{s}}}, \frac{(\epsilon_{\mathrm{s}}C)^{1/2}}{(h\alpha)^{1/2}}\right\}$$

and $|||\cdot|||_1$ is defined in (3.8).

If α is chosen as in equation (3.16), then for $h < h_0$ we find that

$$c = \max\left\{1 + \frac{C}{\epsilon_{\mathrm{s}}}, (\epsilon_{\mathrm{s}}C)^{1/2}\right\}, \tag{3.22}$$

independent of both α and h.

□

3.4. **Error analysis.** We define the error $\widetilde{e} \in \widetilde{\mathcal{V}}$ as the difference between the solution $\psi \in \mathcal{V}$ of the problem (3.3) and the solution $\psi_h \in \mathcal{V}_h$ of the approximated problem (3.7), that is

$$\widetilde{e} = \psi - \psi_h.$$

We perform error estimates for the L^2-norm and the H^1-norm of the error $\widetilde{e}$. Because $a_h(\psi, \phi_h) - a_h(\psi_h, \phi_h) = \ell(\phi_h) - \ell(\phi_h)$, notice that $a_h(\widetilde{e}, \phi_h) = 0$.

We start by estimating the norm $|||\widetilde{e}|||_1$ and then we deduce a relation between $\|\widetilde{e}\|_{L^2_\Omega}$ and $|||\widetilde{e}|||_1$. Since the bilinear form (3.7) is coercive and continuous, we can apply Strang's second lemma (Ciarlet [9]). This lemma ensures that if $\psi \in \mathcal{V}$ is the unique solution of (3.3) and $\psi_h \in \mathcal{V}_h$ is the unique solution of (3.7), then there exists a positive constant $C_1 \in \mathbb{R}$, independent of h, such that

(3.23)
$$|||\widetilde{e}|||_1 = |||\psi - \psi_h|||_1 \leq c_1 \left(\inf_{\phi_h \in \mathcal{V}_h} |||\psi - \phi_h|||_1 + \sup_{\phi_h \in \mathcal{V}_h} \frac{|a_h(\psi, \phi_h) - \ell(\phi_h)|}{|||\phi_h|||_1} \right).$$

Due to Remark 3.1, the last term in (3.23), which is called the *consistency error* of the problem, vanishes. Then, (3.23) reduces to

$$|||\widetilde{e}|||_1 \leq c_1 \inf_{\phi_h \in \mathcal{V}_h} |||\psi - \phi_h|||_1. \tag{3.24}$$

Proposition 3.3 (Error estimates in $|||\cdot|||_1$)**.** *Let k be the order of the B-spline basis approximation, and let $\varphi \in H^{k+1}(\Omega)$. Then*

$$\inf_{\varphi_h \in \mathcal{V}_h} |||\varphi - \varphi_h|||_1 \leq c_2 h^k |\varphi|_{H^{k+1}_\Omega}, \tag{3.25}$$

where the norm $|||\cdot|||_1$ is defined in (3.8)*.*

Proof. From the trace inequality (2.13), (2.9), and (2.10) , we find that

$$\begin{aligned} \|\varphi - \mathcal{I}^h\varphi\|^2_{L^2_\Gamma} &\leq C_1 \left(h^{-1} \|\varphi - \mathcal{I}^h\varphi\|^2_{L^2_\Omega} + h \|\nabla(\varphi - \mathcal{I}^h\varphi)\|^2_{L^2_\Omega} \right) \\ &= C_1 \left(h^{-1} \|\varphi - \mathcal{I}^h\varphi\|^2_{L^2_\Omega} + h |\varphi - \mathcal{I}^h\varphi|^2_{H^1_\Omega} \right) \\ &\leq C_1 \left(h^{-1} h^{2k+2} |\varphi|^2_{H^{k+1}_\Omega} + h h^{2k} |\varphi|^2_{H^{k+1}_\Omega} \right) \\ &= C_2 h^{2k+1} |\varphi|^2_{H^{k+1}_\Omega}. \end{aligned} \tag{3.26}$$

Taking $m = 1$ in (2.9), we obtain the inequality

$$\|\nabla(\varphi - \mathcal{I}^h\varphi)\|^2_{L^2_\Omega} = |\varphi - \mathcal{I}^h\varphi|^2_{H^1_\Omega} \leq C h^{2k} |\varphi|^2_{H^{k+1}_\Omega}. \tag{3.27}$$

Finally using (3.26) and (3.27), we arrive at the estimate

$$\inf_{\varphi_h \in \mathcal{V}_h} |||\varphi - \varphi_h|||^2_1 \leq |||\varphi - \mathcal{I}^h\varphi|||^2_1 \leq \epsilon_{\mathrm{s}} C h^{2k} |\varphi|^2_{H^{k+1}_\Omega} + \alpha C h^{2k+1} |\varphi|^2_{H^{k+1}_\Omega}. \tag{3.28}$$

Choosing α as suggested in (3.17),we obtain (3.25) from (3.28). □

Proposition 3.4 (Error estimates in $||\cdot||_{L^2(\Omega)}$)**.** *Let k be the order of the B-spline basis approximation, and let $\varphi \in H^{k+1}(\Omega)$. Then*

$$||\varphi - \varphi_h||_{L^2(\Omega)} \leq c_3 h^{k+1} |\varphi|_{H^{k+1}_\Omega}. \tag{3.29}$$

Proof. Consider the dual problem: Suppose that it is possible to find $\widetilde{\omega} \in \widetilde{\mathcal{V}}$ such that

$$a_h(\widetilde{\phi}, \widetilde{\omega}) = (\widetilde{e}, \widetilde{\phi}), \qquad \forall\, \widetilde{\phi} \in \widetilde{\mathcal{V}}, \tag{3.30}$$

and assume that this problem is 2-regular, namely that the solution $\tilde{\omega}$ of the problem has the property

$$|\widetilde{\omega}|_{H^2_\Omega} \leq C_{reg} \|\widetilde{e}\|_{L^2_\Omega}. \tag{3.31}$$

On choosing $\widetilde{\phi} = \widetilde{e}$, the dual problem (3.30) gives

$$\|\widetilde{e}\|^2_{L^2_\Omega} = a_h(\widetilde{e}, \widetilde{\omega}). \tag{3.32}$$

Applying the orthogonality of the error and the proposition 3.2 to (3.32) yields

$$\|\widetilde{e}\|^2_{L^2_\Omega} = a_h(\widetilde{e}, \widetilde{\omega} - \omega_h) \leq c|||\widetilde{e}|||_1 \; |||\widetilde{\omega} - \omega_h|||_1, \quad \forall \omega_h \in \mathcal{V}_h.$$

Since $\widetilde{\omega}$ belongs to $\widetilde{\mathcal{V}}$ which is included in H^1_Ω, we can apply Proposition 3.3

$$\|\widetilde{e}\|^2_{L^2_\Omega} \leq c|||\widetilde{e}|||_1 \; |||\widetilde{\omega} - \omega_h|||_1 \leq c|||\widetilde{e}|||_1 \inf_{\phi_h \in \mathcal{V}_h} |||\widetilde{\omega} - \phi_h|||_1 \leq c_1 h |||\widetilde{e}|||_1 \; |\widetilde{\omega}|_{H^2_\Omega}$$

and, by (3.31), we find that

$$\|\widetilde{e}\|^2_{L^2_\Omega} \leq c_2 h |||\widetilde{e}|||_1 \; \|\widetilde{e}\|_{L^2_\Omega}$$

from which it follows that

$$\|\widetilde{e}\|_{L^2_\Omega} \leq c_2 h |||\widetilde{e}|||_1.$$

Finally, from (3.25), we obtain the L^2 error estimate:

$$\|\widetilde{e}\|_{L^2_\Omega} \leq \mathcal{C}_1 h^{k+1} |\psi|_{H^{k+1}_\Omega}. \tag{3.33}$$

□

Proposition 3.5 (Error estimates in $||\cdot||_{H^1(\Omega)}$)**.** *Let k be the order of the B-spline basis approximation, let $\psi \in H^{k+1}_\Omega$ be the solution of the linear Stommel problem, and let $\psi_h \in \mathcal{V}^h$ be the numerical solution. Then*

$$\|\widetilde{e}\|_{H^1_\Omega} \leq c h^k |\psi|_{H^{k+1}_\Omega}. \tag{3.34}$$

Proof. For the H^1-norm of the error, we easily have

$$\|\psi - \psi_h\|_{H^1_\Omega} = \|\psi - \mathcal{I}^h\psi + \mathcal{I}^h\psi - \psi_h\|_{H^1_\Omega} \leq \|\psi - \mathcal{I}^h\psi\|_{H^1_\Omega} + \|\psi_h - \mathcal{I}^h\psi\|_{H^1_\Omega}. \tag{3.35}$$

Using (2.10) with $m = 1$, we obtain the inequality

$$\|\psi - \mathcal{I}^h\psi\|_{H^1_\Omega} \leq c_1 h^k |\psi|_{H^{k+1}_\Omega}. \tag{3.36}$$

Since $\psi_h - \mathcal{I}^h\psi$ belongs to $\mathcal{V}^h$, taking $l = 0$ and $m = 1$ in (2.12) yields the inverse estimate

$$\|\psi_h - \mathcal{I}^h\psi\|_{H^1_\Omega} \leq c_2 h^{-1} \|\psi_h - \mathcal{I}^h\psi\|_{L^2_\Omega}. \tag{3.37}$$

Applying (3.36) and (3.37) in (3.35) yields

$$\begin{aligned}
\|\widetilde{e}\|_{H^1_\Omega} &\leq c_1 h^k |\psi|_{H^{k+1}_\Omega} + c_2 h^{-1} \|\psi_h - \mathcal{I}^h\psi\|_{L^2_\Omega} \\
&= c_1 h^k |\psi|_{H^{k+1}_\Omega} + c_2 h^{-1} \|\psi_h - \psi + \psi - \mathcal{I}^h\psi\|_{L^2_\Omega} \\
&\leq c_1 h^k |\psi|_{H^{k+1}_\Omega} + c_2 h^{-1} (\|\widetilde{e}\|_{L^2_\Omega} + \|\psi - \mathcal{I}^h\psi\|_{L^2_\Omega}).
\end{aligned}$$

The above inequality can be rewritten as

$$\begin{aligned}
\|\widetilde{e}\|_{H^1_\Omega} &\leq c_1 h^k |\psi|_{H^{k+1}_\Omega} + c_2 h^{-1} (\|\widetilde{e}\|_{L^2_\Omega} + c_1 h^{k+1} |\psi|_{H^{k+1}_\Omega}) \\
&\leq c_1 h^k |\psi|_{H^{k+1}_\Omega} + c_2 h^{-1} (\mathcal{C}_1 h^{k+1} |\psi|_{H^{k+1}_\Omega} + c_1 h^{k+1} |\psi|_{H^{k+1}_\Omega}) \\
&= (c_1 + c_2\mathcal{C}_1 + c_2 c_1) h^k |\psi|_{H^{k+1}_\Omega},
\end{aligned}$$

which is the estimate (3.34) with $c = c_1 + c_2\mathcal{C}_1 + c_1c_2$. Here, the last term in the first line is obtained by taking $m = 0$ in (2.10) and (3.33) is applied to the second term in the second line. □

4. The Stommel–Munk Model

The Stommel–Munk model (Vallis [39, eqn. (14.42)]) can be given by

$$\begin{aligned} -\epsilon_{\mathrm{s}}\Delta\psi + \epsilon_{\mathrm{m}}\Delta^2\psi - \frac{\partial\psi}{\partial x} &= F \quad \text{in } \Omega, \\ \psi = 0, \quad \nabla\psi\cdot\mathbf{n} &= 0 \quad \text{on } \Gamma. \end{aligned} \tag{4.1}$$

The parameters ϵ_{s} and ϵ_{m} are the nondimensional Stommel and Munk numbers, respectively, which are defined by

$$\epsilon_{\mathrm{s}} = \frac{\gamma}{\beta L} \quad \text{and} \quad \epsilon_{\mathrm{m}} = \frac{A}{\beta L^3},$$

where γ is the coefficient of the linear drag (or the Rayleigh friction), as might be generated by a bottom Ekman layer, β is the coefficient multiplying the y-coordinate in the β-plane approximation, A is the eddy viscosity parametrization, and L is the characteristic length scale.

4.1. Variational formulation of the Stommel–Munk Model.

The function space of the solution of the problem (4.1) is

$$\mathcal{W} := H_0^2(\Omega) = \left\{\phi \in H_\Omega^2 :\ \phi = \nabla\phi\cdot\mathbf{n} = 0 \quad \text{on } \Gamma\right\}, \tag{4.2}$$

where $H^2(\Omega)$ is the Sobolev space of square integrable functions with square integrable first and second derivatives in Ω. Multiplying $(4.1)_1$ by a test function $\phi \in \mathcal{W}$, integrating by parts twice over Ω, we recover the standard variational formulation of the Stommel–Munk model: Find $\psi \in \mathcal{W}$ such that

$$b(\psi,\phi) = \ell(\phi), \qquad \forall\,\phi \in \mathcal{W}, \tag{4.3}$$

where the bilinear form $b(\cdot,\cdot) : \mathcal{W}\times\mathcal{W} \to \mathbb{R}$ is defined by

$$b(\psi,\phi) = \int_\Omega \epsilon_{\mathrm{s}}\nabla\psi\cdot\nabla\phi\,\mathrm{d}\Omega + \int_\Omega \epsilon_{\mathrm{m}}\Delta\psi\Delta\phi\,\mathrm{d}\Omega - \int_\Omega \frac{\partial\psi}{\partial x}\phi\,\mathrm{d}\Omega \tag{4.4}$$

and

$$\ell(\phi) = \int_\Omega F\phi\,\mathrm{d}\Omega. \tag{4.5}$$

4.2. Nitsche's formulation of the Stommel–Munk model.

The standard variational formulation (4.3) can be used as is for conforming approximations, with boundary conditions being enforced strongly in the space $\mathcal{W}$. As with second-order models, it is possible to use finite-dimensional subspaces of $\mathcal{W}$ based on B-spline basis functions. However, the drawbacks and the complexity in the implementation to strongly enforce the boundary conditions for fourth-order boundary-value problems would be even more pronounced. Here, we provide an analysis of the weaker formulation presented in Kim et al. [29], which proves to be numerically robust.

We consider a finite dimensional space $\mathcal{W}_h$ that is no longer a subspace of $\mathcal{W}$, in the sense that the boundary conditions are no longer imposed strongly in the definition of the space itself. Specifically, functions in $\mathcal{W}_h$ do not satisfy automatically the boundary conditions $(4.1)_2$ and $(4.1)_3$.

As usual in Nitsche-type variational formulation, we define a new function space as the sum

$$\widetilde{\mathcal{W}} = \mathcal{W} + \mathcal{W}_h,$$

where $\mathcal{W}$ is defined in (4.2) and $\mathcal{W}_h$ is defined in (2.16). We approximate (4.3) by the stabilised finite dimensional variational problem: Find $\psi_h \in \mathcal{W}_h$ such that

$$b_h(\psi_h, \phi_h) = \ell(\phi_h), \qquad \forall\, \phi_h \in \mathcal{W}_h, \tag{4.6}$$

where the stabilized bilinear form $b_h(\cdot,\cdot) : \widetilde{\mathcal{W}} \times \widetilde{\mathcal{W}} \to \mathbb{R}$ is defined by

(4.7)

$$\begin{aligned} b_h(\widetilde{\psi},\widetilde{\phi}) = &\int_\Omega \epsilon_{\mathrm{s}} \nabla\widetilde{\psi}\cdot\nabla\widetilde{\phi}\,\mathrm{d}\Omega + \int_\Omega \epsilon_{\mathrm{m}}\Delta\widetilde{\psi}\Delta\widetilde{\phi}\,\mathrm{d}\Omega - \int_\Omega \frac{\partial\widetilde{\psi}}{\partial x}\widetilde{\phi}\,\mathrm{d}\Omega \\ &- \int_\Gamma \epsilon_{\mathrm{s}}(\nabla\widetilde{\psi}\cdot\mathbf{n})\widetilde{\phi}\,\mathrm{d}\Gamma - \int_\Gamma \epsilon_{\mathrm{s}}(\nabla\widetilde{\phi}\cdot\mathbf{n})\widetilde{\psi}\,\mathrm{d}\Gamma + \int_\Gamma \epsilon_{\mathrm{m}}\widetilde{\phi}(\nabla(\Delta\widetilde{\psi})\cdot\mathbf{n})\,\mathrm{d}\Gamma \\ &+ \int_\Gamma \epsilon_{\mathrm{m}}\widetilde{\psi}(\nabla(\Delta\widetilde{\phi})\cdot\mathbf{n})\,\mathrm{d}\Gamma + \alpha_1\int_\Gamma \widetilde{\psi}\widetilde{\phi}\,\mathrm{d}\Gamma \\ &- \int_\Gamma \epsilon_{\mathrm{m}}(\nabla\widetilde{\phi}\cdot\mathbf{n})\Delta\widetilde{\psi}\,\mathrm{d}\Gamma - \int_\Gamma \epsilon_{\mathrm{m}}(\nabla\widetilde{\psi}\cdot\mathbf{n})\Delta\widetilde{\phi}\,\mathrm{d}\Gamma + \alpha_2\int_\Gamma (\nabla\widetilde{\phi}\cdot\mathbf{n})(\nabla\widetilde{\psi}\cdot\mathbf{n})\,\mathrm{d}\Gamma \end{aligned}$$

and

$$\ell(\widetilde{\phi}) = \int_\Omega F\widetilde{\phi}\,\mathrm{d}\Omega.$$

The parameters α_1 and α_2 in (4.7) are two mesh-dependent stabilization parameters, which will be specified later. Notice that if we choose ψ and ϕ in the space $\mathcal{W}$, then the bilinear form b_h in (4.7) coincides with the form b in (4.4) since all integrals on the boundary Γ vanish.

The second, third and fourth lines in (4.7) make it possible to impose weakly the boundary conditions $\psi = 0$ and $\nabla\psi\cdot\mathbf{n} = 0$ while maintaining consistency with the solution of the original formulation (4.3), as summarised in the following remark:

Remark 4.1. *If we multiply* $(4.1)_1$ *by a test function* $\phi_h \in \mathcal{W}_h$*, integrate by parts and take into account the boundary conditions* $(4.1)_2$ *and* $(4.1)_3$ *on* $\psi \in \mathcal{W}$*, we find that*

$$\begin{aligned} \int_\Omega \epsilon_s\nabla\psi\cdot\nabla\phi_h\,d\Omega + &\int_\Omega \epsilon_m\Delta\psi\Delta\phi_h\,d\Omega - \int_\Gamma \epsilon_m(\nabla\phi_h\cdot\mathbf{n})\Delta\psi\,d\Gamma \\ &+ \int_\Gamma \epsilon_m(\nabla(\Delta\psi)\cdot\mathbf{n})\phi_h\,d\Gamma - \int_\Omega \frac{\partial\psi}{\partial x}\phi_h\,d\Omega = \int_\Omega F\phi_h\,d\Omega, \end{aligned}$$

which, from (4.7) *and* (4.5)*, implies that*

$$b_h(\psi,\phi_h) - \ell(\phi_h) = 0.$$

As with the Stommel model, the bilinear form b_h in (4.7) suggests the definition of a mesh-dependent norm in $\widetilde{\mathcal{W}}$, with respect to which we can prove coercivity, continuity, and convergence of the numerical method:

$$|||\widetilde{\psi}|||_2^2 := \|\epsilon_{\mathrm{m}}^{1/2}\Delta\widetilde{\psi}\|_{L^2_\Omega}^2 + \|\epsilon_{\mathrm{s}}^{1/2}\nabla\widetilde{\psi}\|_{L^2_\Omega}^2 + \|\alpha_1^{1/2}\widetilde{\psi}\|_{L^2_\Gamma}^2 + \|\alpha_2^{1/2}\nabla\widetilde{\psi}\cdot\mathbf{n}\|_{L^2_\Gamma}^2. \tag{4.8}$$

4.3. Ellipticity and continuity of the bilinear form b_h.

Proposition 4.1. *It is possible to choose the stabilization parameters* α_1 *and* α_2 *such that the bilinear form* (4.7) *is uniformly* $\mathcal{W}_h$*-elliptic, namely for which there exists a constant* $M > 0$ *such that*

$$b_h(\psi_h,\psi_h) \geq M|||\psi_h|||_2^2, \quad \forall\psi_h \in \mathcal{W}_h$$

where M *is independent of* h*,* α_1*, and* α_2*.*

Proof. Replacing both $\widetilde{\psi}$ and $\widetilde{\phi}$ by ψ_h in (4.7) yields

(4.9)
$$\begin{aligned} b_h(\psi_h,\psi_h) =& \|\epsilon_{\mathrm{s}}^{1/2}\nabla\psi_h\|_{L^2_\Omega}^2 + \|\epsilon_{\mathrm{m}}^{1/2}\Delta\psi_h\|_{L^2_\Omega}^2 + \|\alpha_1^{1/2}\psi_h\|_{L^2_\Gamma}^2 + \|\alpha_2^{1/2}\nabla\psi_h\cdot\mathbf{n}\|_{L^2_\Gamma}^2 \\ &- 2\int_\Gamma \epsilon_{\mathrm{s}}(\nabla\psi_h\cdot\mathbf{n})\psi_h\,\mathrm{d}\Gamma + 2\int_\Gamma \epsilon_{\mathrm{m}}\psi_h(\nabla(\Delta\psi_h)\cdot\mathbf{n})\,\mathrm{d}\Gamma \\ &- 2\int_\Gamma \epsilon_{\mathrm{m}}(\nabla\psi_h\cdot\mathbf{n})\Delta\psi_h\,\mathrm{d}\Gamma - \int_\Omega \frac{\partial\psi_h}{\partial x}\psi_h\,\mathrm{d}\Omega. \end{aligned}$$

Applying Young's inequality (3.12) and the inequality (3.9) to the first term of the second line of (4.9) results in

$$-2\int_\Gamma \epsilon_{\mathrm{s}}(\nabla\psi_h\cdot\mathbf{n})\psi_h\,\mathrm{d}\Gamma \geq -\delta_1\epsilon_{\mathrm{s}}C_1h^{-1}\|\epsilon_{\mathrm{s}}^{1/2}\nabla\psi_h\|_{L^2_\Omega}^2 - \frac{1}{\delta_1\alpha_1}\|\alpha_1^{1/2}\psi_h\|_{L^2_\Gamma}^2, \tag{4.10}$$

where C_1 is a positive constant.

The second term of the second line in (4.9) can be integrated by parts over Γ to obtain

$$\int_\Gamma \epsilon_{\mathrm{m}}\psi_h(\nabla(\Delta\psi_h)\cdot\mathbf{n})\,\mathrm{d}\Gamma = -\int_\Gamma \epsilon_{\mathrm{m}}(\nabla\psi_h\cdot\mathbf{n})\,\Delta\psi_h\,\mathrm{d}\Gamma. \tag{4.11}$$

Since Γ is closed the co-dimension two boundary integral term in (4.11) vanishes.

On using (4.11), (4.9) can be rewritten as

(4.12)
$$\begin{aligned} b_h(\psi_h,\psi_h) =& \|\epsilon_{\mathrm{s}}^{1/2}\nabla\psi_h\|_{L^2_\Omega}^2 + \|\epsilon_{\mathrm{m}}^{1/2}\Delta\psi_h\|_{L^2_\Omega}^2 + \|\alpha_1^{1/2}\psi_h\|_{L^2_\Gamma}^2 + \|\alpha_2^{1/2}\nabla\psi_h\cdot\mathbf{n}\|_{L^2_\Gamma}^2 \\ &- 2\int_\Gamma \epsilon_{\mathrm{s}}(\nabla\psi_h\cdot\mathbf{n})\psi_h\,\mathrm{d}\Gamma - 4\int_\Gamma \epsilon_{\mathrm{m}}(\nabla\psi_h\cdot\mathbf{n})\Delta\psi_h\,\mathrm{d}\Gamma \\ &- \int_\Omega \frac{\partial\psi_h}{\partial x}\psi_h\,\mathrm{d}\Omega. \end{aligned}$$

Moreover, we can apply (2.14) to the function $\Delta\psi_h$ to yield

$$\|\Delta\psi_h\|_{L^2_\Gamma}^2 \leq C_2h^{-1}\|\Delta\psi_h\|_{L^2_\Omega}^2.$$

Then, on using Young's inequality (3.12), the second term of the second line in (4.12) yields

(4.13)
$$-4\int_\Gamma \epsilon_{\mathrm{m}}(\nabla\psi_h\cdot\mathbf{n})\Delta\psi_h\,\mathrm{d}\Gamma \geq -2\delta_2\epsilon_{\mathrm{m}}C_2h^{-1}\|\epsilon_{\mathrm{m}}^{1/2}\Delta\psi_h\|_{L^2_\Omega}^2 - \frac{2}{\delta_2\alpha_2}\|\alpha_2^{1/2}\nabla\psi_h\cdot\mathbf{n}\|_{L^2_\Gamma}^2,$$

where C_2 and δ_2 are positive constants.

Finally, we use the inequality (3.15) in the last term of (4.12). By substituting the inequalities (3.15), (4.10), and (4.13) into (4.12), we obtain

$$\begin{aligned} b_h(\psi_h,\psi_h) &\geq \|\epsilon_{\rm s}^{1/2}\nabla\psi_h\|^2_{L^2_\Omega} + \|\epsilon_{\rm m}^{1/2}\Delta\psi_h\|^2_{L^2_\Omega} + \|\alpha_1^{1/2}\psi_h\|^2_{L^2_\Gamma} + \|\alpha_2^{1/2}\nabla\psi_h\cdot\mathbf{n}\|^2_{L^2_\Gamma} \\ &\quad - \frac{1}{2\alpha_1}\|\alpha_1^{1/2}\psi_h\|^2_{L^2_\Gamma} - \delta_1\epsilon_{\rm s}C_1h^{-1}\|\epsilon_{\rm s}^{1/2}\nabla\psi_h\|^2_{L^2_\Omega} - \frac{1}{\delta_1\alpha_1}\|\alpha_1^{1/2}\psi_h\|^2_{L^2_\Gamma} \\ &\quad - 2\delta_2\epsilon_{\rm m}C_2h^{-1}\|\epsilon_{\rm m}^{1/2}\Delta\psi_h\|^2_{L^2_\Omega} - \frac{2}{\delta_2\alpha_2}\|\alpha_2^{1/2}\nabla\psi_h\cdot\mathbf{n}\|^2_{L^2_\Gamma} \\ &\geq m_1\|\epsilon_{\rm s}^{1/2}\nabla\psi_h\|^2_{L^2_\Omega} + m_2\|\epsilon_{\rm m}^{1/2}\Delta\psi_h\|^2_{L^2_\Omega} + m_3\|\alpha_1^{1/2}\psi_h\|^2_{L^2_\Gamma} + m_4\|\alpha_2^{1/2}\nabla\psi_h\cdot\mathbf{n}\|^2_{L^2_\Gamma} \\ &\geq M|||\psi_h|||_2^2, \end{aligned}$$

where

$$m_1 = 1 - \frac{\delta_1\epsilon_{\rm s}C_1}{h}, \qquad m_2 = 1 - \frac{2\delta_2\epsilon_{\rm m}C_2}{h},$$

$$m_3 = 1 - \frac{1}{2\alpha_1} - \frac{1}{\alpha_1\delta_1}, \qquad m_4 = 1 - \frac{2}{\delta_2\alpha_2},$$

and M is a positive constant.

If we we choose δ_1, δ_2, α_1, and α_2 such that m_1, m_2, m_3 and m_4 are equal (to $M > 0$), we find that $\delta_2 = \delta_1\epsilon_{\rm s}C_1/(2C_2\epsilon_{\rm m})$. Moreover, the positivity of m_1 is guaranteed if $\delta_1 < h/(\epsilon_{\rm s}C_1)$. Taking

$$\delta_1 = \frac{r}{\epsilon_{\rm s}C_1}\,h \quad \text{with} \quad r \in (0,1)$$

yields $\delta_2 = rh/(2C_2\epsilon_{\rm m})$,

$$\alpha_1 = \frac{1}{2r} + \frac{\epsilon_{\rm s}C_1}{r^2}\,h^{-1}, \qquad \alpha_2 = \frac{4\epsilon_{\rm m}C_2}{r^2}\,h^{-1}, \tag{4.14}$$

and the constant M is equal to $1-r$, which is independent of h, α_1, and α_2. □

Let h_0 be chosen so that $\frac{\epsilon_{\rm s}C_1}{r^2}h_0^{-1} >> \frac{1}{2r}$. Then, for $h < h_0$, (4.14) indicates that the stabilization parameters α_1 and α_2 are mesh-dependent and their asymptotic behaviour when $h \to 0$ is given by

$$\alpha_1 \sim \frac{1}{h} \quad \text{and} \quad \alpha_2 \sim \frac{1}{h}. \tag{4.15}$$

Proposition 4.2. *If we choose the stabilization parameters as in equation* (4.14)*, then the bilinear form* (4.7) *is uniformly continuous in* $\widetilde{\mathcal{W}}$*, namely there exists a constant* $c < \infty$ *such that*

$$\left|b_h(\widetilde{\psi},\widetilde{\phi})\right| \leq c|||\widetilde{\psi}|||_2\;|||\widetilde{\phi}|||_2,$$

where the norm $|||\cdot|||_2$ *is defined in* (4.8) *and* c *is independent on* α_1*,* α_2*, and* h*.*

Proof. By definition of the bilinear form b_h we have

(4.16)
$$\begin{aligned}\left|b_h(\widetilde{\psi},\widetilde{\phi})\right| \le & \int_\Omega \left|\epsilon_{\mathrm{s}}\nabla\widetilde{\psi}\cdot\nabla\widetilde{\phi}\right| \,\mathrm{d}\Omega + \int_\Omega \left|\epsilon_{\mathrm{m}}\Delta\widetilde{\psi}\Delta\widetilde{\phi}\right| \,\mathrm{d}\Omega + \int_\Omega \left|\frac{\partial\widetilde{\psi}}{\partial x}\widetilde{\phi}\right| \,\mathrm{d}\Omega \\ & + \int_\Gamma \left|\epsilon_{\mathrm{s}}(\nabla\widetilde{\psi}\cdot\mathbf{n})\widetilde{\phi}\right| \,\mathrm{d}\Gamma + \int_\Gamma \left|\epsilon_{\mathrm{s}}(\nabla\widetilde{\phi}\cdot\mathbf{n})\widetilde{\psi}\right| \,\mathrm{d}\Gamma + \left|\int_\Gamma \epsilon_{\mathrm{m}}\widetilde{\phi}(\nabla(\Delta\widetilde{\psi})\cdot\mathbf{n})\,\mathrm{d}\Gamma\right| \\ & + \left|\int_\Gamma \epsilon_{\mathrm{m}}\widetilde{\psi}(\nabla(\Delta\widetilde{\phi})\cdot\mathbf{n})\,\mathrm{d}\Gamma\right| + \alpha_1\int_\Gamma \left|\widetilde{\psi}\widetilde{\phi}\right| \,\mathrm{d}\Gamma \\ & + \int_\Gamma \left|\epsilon_{\mathrm{m}}(\nabla\widetilde{\phi}\cdot\mathbf{n})\Delta\widetilde{\psi}\,\mathrm{d}\Gamma\right| + \int_\Gamma \left|\epsilon_{\mathrm{m}}(\nabla\widetilde{\psi}\cdot\mathbf{n})\Delta\widetilde{\phi}\right| \,\mathrm{d}\Gamma \\ & + \alpha_2\int_\Gamma \left|(\nabla\widetilde{\phi}\cdot\mathbf{n})(\nabla\widetilde{\psi}\cdot\mathbf{n})\right| \,\mathrm{d}\Gamma.\end{aligned}$$

Applying Hölder's inequality and the trace theorem to the first two integrals on the second line of (4.16) yields

$$\begin{aligned}\int_\Gamma \epsilon_{\mathrm{s}}(\nabla\widetilde{\psi}\cdot\mathbf{n})\widetilde{\phi}\,\mathrm{d}\Gamma &\le \frac{\epsilon_{\mathrm{s}}^{1/2}}{\alpha_1^{1/2}}\|\epsilon_{\mathrm{s}}^{1/2}\nabla\widetilde{\psi}\|_{L^2_\Gamma}\|\alpha_1^{1/2}\widetilde{\phi}\|_{L^2_\Gamma} \\ &\le \frac{(C\epsilon_{\mathrm{s}})^{1/2}}{(h\alpha_1)^{1/2}}\|\epsilon_{\mathrm{s}}^{1/2}\nabla\widetilde{\psi}\|_{L^2_\Omega}\|\alpha_1^{1/2}\widetilde{\phi}\|_{L^2_\Gamma}\end{aligned} \tag{4.17}$$

and, in the same way,

$$\int_\Gamma \epsilon_{\mathrm{s}}(\nabla\widetilde{\phi}\cdot\mathbf{n})\widetilde{\psi}\,\mathrm{d}\Gamma \le \frac{(C\epsilon_{\mathrm{s}})^{1/2}}{(h\alpha_1)^{1/2}}\|\epsilon_{\mathrm{s}}^{1/2}\nabla\widetilde{\phi}\|_{L^2_\Omega}\|\alpha_1^{1/2}\widetilde{\psi}\|_{L^2_\Gamma}, \tag{4.18}$$

where C is a positive constant.

Substituting (4.17) and (4.18) into (4.16), we obtain

$$\begin{aligned}\left|b_h(\widetilde{\psi},\widetilde{\phi})\right| \le & \|\epsilon_{\mathrm{s}}^{1/2}\nabla\widetilde{\psi}\|_{L^2_\Omega}\|\epsilon_{\mathrm{s}}^{1/2}\nabla\widetilde{\phi}\|_{L^2_\Omega} + \|\epsilon_{\mathrm{m}}^{1/2}\Delta\widetilde{\psi}\|_{L^2_\Omega}\|\epsilon_{\mathrm{m}}^{1/2}\Delta\widetilde{\phi}\|_{L^2_\Omega} \\ & + \frac{(C\epsilon_{\mathrm{s}})^{1/2}}{(h\alpha_1)^{1/2}}\left[\|\epsilon_{\mathrm{s}}^{1/2}\nabla\widetilde{\psi}\|_{L^2_\Omega}\|\alpha_1^{1/2}\widetilde{\phi}\|_{L^2_\Gamma} + \|\epsilon_{\mathrm{s}}^{1/2}\nabla\widetilde{\phi}\|_{L^2_\Omega}\|\alpha_1^{1/2}\widetilde{\psi}\|_{L^2_\Gamma}\right] \\ & + \|\alpha_1^{1/2}\widetilde{\psi}\|_{L^2_\Gamma}\|\alpha_1^{1/2}\widetilde{\phi}\|_{L^2_\Gamma} + \|\alpha_2^{1/2}\nabla\widetilde{\psi}\cdot\mathbf{n}\|_{L^2_\Gamma}\|\alpha_2^{1/2}\nabla\widetilde{\phi}\cdot\mathbf{n}\|_{L^2_\Gamma} \\ & + \|\epsilon_{\mathrm{s}}^{1/2}\nabla\widetilde{\psi}\|_{L^2_\Omega}\left(\frac{C}{\epsilon_{\mathrm{s}}}\|\epsilon_{\mathrm{s}}^{1/2}\nabla\widetilde{\phi}\|_{L^2_\Omega} + \frac{C_3}{h\alpha_1}\|\alpha_1^{1/2}\widetilde{\phi}\|_{L^2_\Gamma}\right) \\ & + \left|\int_\Gamma \epsilon_{\mathrm{m}}\widetilde{\phi}(\nabla(\Delta\widetilde{\psi})\cdot\mathbf{n})\,\mathrm{d}\Gamma\right| + \left|\int_\Gamma \epsilon_{\mathrm{m}}\widetilde{\psi}(\nabla(\Delta\widetilde{\phi})\cdot\mathbf{n})\,\mathrm{d}\Gamma\right| \\ & + \int_\Gamma \left|\epsilon_{\mathrm{m}}(\nabla\widetilde{\phi}\cdot\mathbf{n})\Delta\widetilde{\psi}\right| \,\mathrm{d}\Gamma + \int_\Gamma \left|\epsilon_{\mathrm{m}}(\nabla\widetilde{\psi}\cdot\mathbf{n})\Delta\widetilde{\phi}\right| \,\mathrm{d}\Gamma,\end{aligned} \tag{4.19}$$

where Hölder's inequality and Lemma 3.2 have been used in the first, third, and fourth lines.

We integrate by parts the first two integrals in (4.19)

$$\left|\int_\Gamma \epsilon_{\mathrm{m}}\widetilde{\phi}(\nabla(\Delta\widetilde{\psi})\cdot\mathbf{n})\,\mathrm{d}\Gamma\right| = \left|\int_\Gamma \epsilon_{\mathrm{m}}(\nabla\widetilde{\phi}\cdot\mathbf{n})\Delta\widetilde{\psi}\,\mathrm{d}\Gamma\right| \leq \int_\Gamma \left|\epsilon_{\mathrm{m}}(\nabla\widetilde{\phi}\cdot\mathbf{n})\Delta\widetilde{\psi}\right|\,\mathrm{d}\Gamma, \tag{4.20}$$

and, since Γ is closed the co-dimension two boundary integral term vanishes.

If $\widetilde{\psi}$ and $\widetilde{\phi}$ belong to $\mathcal{W}$ integrals in (4.19) vanish and the bilinear form b_h is equivalent to the form b defined in (4.4). We can restrict $\widetilde{\psi}$ and $\widetilde{\phi}$ to $\mathcal{W}_h$ and we can apply inverse estimates from section 2.1. By (4.20), using the trace inequality and Hölder's inequality, we obtain

$$\left|\int_\Gamma \epsilon_{\mathrm{m}}\widetilde{\phi}(\nabla(\Delta\widetilde{\psi})\cdot\mathbf{n})\,\mathrm{d}\Gamma\right| \leq \int_\Gamma \left|\epsilon_{\mathrm{m}}(\nabla\widetilde{\phi}\cdot\mathbf{n})\Delta\widetilde{\psi}\right|\,\mathrm{d}\Gamma \leq \frac{(\epsilon_{\mathrm{m}}C)^{1/2}}{(h\alpha_1)^{1/2}}\|\epsilon_{\mathrm{m}}^{1/2}\Delta\widetilde{\psi}\|_{L^2_\Omega}\|\alpha_1^{1/2}\widetilde{\phi}\|_{L^2_\Gamma},$$

and, in the same way,

$$\left|\int_\Gamma \epsilon_{\mathrm{m}}\widetilde{\psi}(\nabla(\Delta\widetilde{\phi})\cdot\mathbf{n})\,\mathrm{d}\Gamma\right| \leq \int_\Gamma \left|\epsilon_{\mathrm{m}}(\nabla\widetilde{\psi}\cdot\mathbf{n})\Delta\widetilde{\phi}\right|\,\mathrm{d}\Gamma \leq \frac{(\epsilon_{\mathrm{m}}C)^{1/2}}{(h\alpha_1)^{1/2}}\|\epsilon_{\mathrm{m}}^{1/2}\Delta\widetilde{\phi}\|_{L^2_\Omega}\|\alpha_1^{1/2}\widetilde{\psi}\|_{L^2_\Gamma},$$

for all $\widetilde{\phi}$ and $\widetilde{\psi}$ in $\mathcal{W}+\mathcal{W}_h$.

Then, on using Young's inequality and (3.9), (4.19) becomes

$$\begin{aligned}
b_h(\widetilde{\psi},\widetilde{\phi}) \leq & \|\epsilon_{\mathrm{s}}^{1/2}\nabla\widetilde{\psi}\|_{L^2_\Omega}\|\epsilon_{\mathrm{s}}^{1/2}\nabla\widetilde{\phi}\|_{L^2_\Omega} + \|\epsilon_{\mathrm{m}}^{1/2}\Delta\widetilde{\psi}\|_{L^2_\Omega}\|\epsilon_{\mathrm{m}}^{1/2}\Delta\widetilde{\phi}\|_{L^2_\Omega} \\
& + \frac{(\epsilon_{\mathrm{s}}C)^{1/2}}{(h\alpha_1)^{1/2}}\left[\|\epsilon_{\mathrm{s}}^{1/2}\nabla\widetilde{\psi}\|_{L^2_\Omega}\|\alpha_1^{1/2}\widetilde{\phi}\|_{L^2_\Gamma} + \|\epsilon_{\mathrm{s}}^{1/2}\nabla\widetilde{\phi}\|_{L^2_\Omega}\|\alpha_1^{1/2}\widetilde{\psi}\|_{L^2_\Gamma}\right] \\
& + \left(1+\frac{1}{\alpha_1}\right)\|\alpha_1^{1/2}\widetilde{\psi}\|_{L^2_\Gamma}\|\alpha_1^{1/2}\widetilde{\phi}\|_{L^2_\Gamma} + \|\alpha_2^{1/2}\nabla\widetilde{\psi}\cdot\mathbf{n}\|_{L^2_\Gamma}\|\alpha_2^{1/2}\nabla\widetilde{\phi}\cdot\mathbf{n}\|_{L^2_\Gamma} \\
& + \frac{(\epsilon_{\mathrm{m}}C)^{1/2}}{(h\alpha_1)^{1/2}}\left[\|\epsilon_{\mathrm{m}}^{1/2}\Delta\widetilde{\psi}\|_{L^2_\Omega}\|\alpha_1^{1/2}\widetilde{\phi}\|_{L^2_\Gamma} + \|\epsilon_{\mathrm{m}}^{1/2}\Delta\widetilde{\phi}\|_{L^2_\Omega}\|\alpha_1^{1/2}\widetilde{\psi}\|^2_{L^2_\Gamma}\right] \\
& + \frac{(\epsilon_{\mathrm{m}}C)^{1/2}}{(h\alpha_2)^{1/2}}\left[\|\epsilon_{\mathrm{m}}^{1/2}\Delta\widetilde{\psi}\|_{L^2_\Omega}\|\alpha_2^{1/2}\nabla\widetilde{\phi}\cdot\mathbf{n}\|_{L^2_\Gamma} + \|\epsilon_{\mathrm{m}}^{1/2}\Delta\widetilde{\phi}\|_{L^2_\Omega}\|\alpha_2^{1/2}\nabla\widetilde{\psi}\cdot\mathbf{n}\|_{L^2_\Gamma}\right] \\
\leq & c\left(\|\epsilon_{\mathrm{s}}^{1/2}\nabla\widetilde{\psi}\|_{L^2_\Omega} + \|\epsilon_{\mathrm{m}}^{1/2}\Delta\widetilde{\psi}\|_{L^2_\Omega} + \|\alpha_1^{1/2}\widetilde{\psi}\|_{L^2_\Gamma} + \|\alpha_2^{1/2}\nabla\widetilde{\psi}\cdot\mathbf{n}\|_{L^2_\Gamma}\right) \\
& \left(\|\epsilon_{\mathrm{s}}^{1/2}\nabla\widetilde{\phi}\|_{L^2_\Omega} + \|\epsilon_{\mathrm{m}}^{1/2}\Delta\widetilde{\phi}\|_{L^2_\Omega} + \|\alpha_1^{1/2}\widetilde{\phi}\|_{L^2_\Gamma} + \|\alpha_2^{1/2}\nabla\widetilde{\phi}\cdot\mathbf{n}\|_{L^2_\Gamma}\right) \\
\leq & c|||\widetilde{\psi}|||_2\;|||\widetilde{\phi}|||_2,
\end{aligned}$$

where c is determined by

$$c = \max\left\{\frac{(\epsilon_{\mathrm{s}}C)^{1/2}}{(h\alpha_1)^{1/2}}, 1+\frac{1}{\alpha_1}, \frac{(\epsilon_{\mathrm{m}}C)^{1/2}}{(h\alpha_1)^{1/2}}, \frac{(\epsilon_{\mathrm{m}}C)^{1/2}}{(h\alpha_2)^{1/2}}\right\}.$$

If α_1 and α_2 are chosen as in equation (4.14), then for $h < h_0$ we have

$$c = \max\left\{(\epsilon_{\mathrm{s}}\tilde{C})^{1/2}, 1+h_0, (\epsilon_{\mathrm{m}}\tilde{C})^{1/2}, (\epsilon_{\mathrm{m}}\tilde{C})^{1/2}\right\},$$

independent of α_1, α_2, and h.

□

4.4. **Error analysis for the Stommel-Munk model.** We define the error $\widetilde{e} \in \widetilde{\mathcal{W}}$ as the difference

$$\widetilde{e} = \psi - \psi_h,$$

between the solution $\psi \in \mathcal{W}$ of the problem (4.3) and the solution $\psi_h \in \mathcal{W}_h$ of the approximated problem (4.6). Because $b_h(\psi,\phi_h) - b_h(\psi_h,\phi_h) = \ell(\phi_h) - \ell(\phi_h) = 0$, it follows that the $\tilde{e}$ and ϕ_h are orthogonal in the sense that $b_h(\tilde{e},\phi_h) = 0$. Using the

coercivity and the continuity of the bilinear form b_h, we can apply Strang's second lemma to find that there exists a positive constant $C_3 \in \mathbb{R}$, independent of h, such that

(4.21)
$$|||\widetilde{e}|||_2 = |||\psi - \psi_h|||_2 \leq C_3 \left(\inf_{\phi_h \in \mathcal{W}_h} |||\psi - \phi_h|||_2 + \sup_{\phi_h \in \mathcal{W}_h} \frac{|b_h(\psi, \phi_h) - \ell(\phi_h)|}{|||\phi_h|||_2} \right),$$

with ψ and ψ_h being unique solutions of the problems (4.3) and (4.6), respectively. Due to Remark 4.1, the second term in (4.21) vanishes. Using (2.9) with $m = 2$, we obtain the inequality

$$\|\Delta(\psi - \mathcal{I}^h\psi)\|_{L^2_\Omega} \leq |\psi - \mathcal{I}^h\psi|_{H^2_\Omega} \leq Ch^{k-1}|\psi|_{H^{k+1}_\Omega} \qquad \forall \psi \in H^{k+1}_\Omega. \tag{4.22}$$

From the trace theorem (2.13) we have

$$\begin{aligned}
\|\nabla(\psi - \mathcal{I}^h\psi) \cdot \mathbf{n}\|^2_{L^2_\Gamma} &\leq \|\nabla(\psi - \mathcal{I}^h\psi)\|^2_{L^2_\Gamma} \\
&\leq C_4 \left(h^{-1}\|\nabla(\psi - \mathcal{I}^h\psi)\|^2_{L^2_\Omega} + h\|\nabla(\psi - \mathcal{I}^h\psi)\|^2_{H^1_\Omega} \right) \\
&\leq C_4 \left(h^{-1}|\psi - \mathcal{I}^h\psi|^2_{H^1_\Omega} + h|\psi - \mathcal{I}^h\psi|^2_{H^2_\Omega} \right) \\
&\leq C_4 \left(h^{-1}h^{2k}|\psi|^2_{H^{k+1}_\Omega} + hh^{2k-2}|\psi|^2_{H^{k+1}_\Omega} \right) \\
&\leq C_5 h^{2k-1}|\psi|^2_{H^{k+1}_\Omega},
\end{aligned} \tag{4.23}$$

where the third line is obtained from (2.9) by taking $m = 1$ for the first term and $m = 2$ for the second term.

Using (2.13), (2.10), (4.22), and (4.23), we obtain the estimate

(4.24)
$$\begin{aligned}
\inf_{\phi_h \in \mathcal{W}_h} |||\psi - \phi_h|||^2_2 &\leq |||\psi - \mathcal{I}^h\psi|||^2_2 \\
&\leq (\epsilon_{\mathrm{s}} C_3 h^{2k} + \epsilon_{\mathrm{m}} C h^{2k-2} + \alpha_1 C_5 h^{2k+1} + \alpha_2 C_5 h^{2k-1})|\psi|^2_{H^{k+1}_\Omega} \\
&\leq (\epsilon_{\mathrm{s}} C_3 h^{2k} + \epsilon_{\mathrm{m}} C h^{2k-2} + C_5 h^{2k} + C_5 h^{2k-2})|\psi|^2_{H^{k+1}_\Omega}
\end{aligned}$$

where we used (4.15); then if h is small enough we obtain to leading order

$$\inf_{\phi_h \in \mathcal{W}_h} |||\psi - \phi_h|||_2 \leq \widetilde{C} h^{k-1}|\psi|_{H^{k+1}_\Omega}$$

which means that

$$|||\widetilde{e}|||_2 \leq \widetilde{C}_1 h^{k-1}|\psi|_{H^{k+1}_\Omega}. \tag{4.25}$$

We consider the dual problem: Find $\widetilde{\omega} \in \widetilde{\mathcal{W}}$ such that

$$b_h(\widetilde{\phi}, \widetilde{\omega}) = (\widetilde{e}, \widetilde{\phi}), \qquad \forall\, \widetilde{\phi} \in \widetilde{\mathcal{W}}. \tag{4.26}$$

We assume that it is 4-regular, i.e., $|\widetilde{\omega}|_{H^4_\Omega} \leq c_r \|\widetilde{e}\|_{L^2_\Omega}$. Choosing $\widetilde{\phi} = \widetilde{e}$, the dual problem (4.26) gives

$$\|\widetilde{e}\|^2_{L^2_\Omega} = b_h(\widetilde{e}, \widetilde{\omega}).$$

Using the orthogonality of the error and proposition 4.2, we find that

$$\|\widetilde{e}\|^2_{L^2_\Omega} = b_h(\widetilde{e}, \widetilde{\omega} - \omega_h) \leq c|||\widetilde{e}|||_2 \, |||\widetilde{\omega} - \omega_h|||_2, \quad \forall \omega_h \in \mathcal{V}_h. \tag{4.27}$$

From (3.25) and 4-regularity of the dual problem, we notice that

$$\|\widetilde{e}\|^2_{L^2_\Omega} \leq c_1 h|||\widetilde{e}|||_2 \, |\widetilde{\omega}|_{H^4_\Omega} \leq c_2 h^2 |||\widetilde{e}|||_2 \, \|\widetilde{e}\|_{L^2_\Omega}. \tag{4.28}$$

Thus,

$$\|\widetilde{e}\|_{L^2_\Omega} \leq c_2 h^2 |||\widetilde{e}|||_2. \tag{4.29}$$

Finally from (4.25), we obtain the L^2-norm error estimate

$$\|\widetilde{e}\|_{L^2_\Omega} \leq \mathcal{C}_1 h^{k+1} |\psi|_{H^{k+1}(\Omega)}. \tag{4.30}$$

Moreover we can get the error estimate in the H^1-norm and H^2-norm using the following proposition:

Proposition 4.3. *Let $\psi \in H^{k+1}_\Omega$ be the solution of the linear Stommel–Munk problem and let $\psi_h \in \mathcal{W}^h$ a numerical approximation to ψ. Then,*

$$\|\widetilde{e}\|_{H^1_\Omega} \leq c_3 h^k |\psi|_{H^{k+1}_\Omega} \tag{4.31}$$

and

$$\|\widetilde{e}\|_{H^2_\Omega} \leq c_4 h^{k-1} |\psi|_{H^{k+1}_\Omega}. \tag{4.32}$$

Proof. The estimate in (4.31) is established in the proof of Proposition 3.5. For the error in (4.32) we have

$$\|\psi - \psi_h\|_{H^2_\Omega} = \|\psi - \mathcal{I}^h\psi + \mathcal{I}^h\psi - \psi_h\|_{H^2_\Omega} \leq \|\psi - \mathcal{I}^h\psi\|_{H^2_\Omega} + \|\psi_h - \mathcal{I}^h\psi\|_{H^2_\Omega}. \tag{4.33}$$

Using (2.10) we have

$$\|\psi - \mathcal{I}^h\psi\|_{H^2_\Omega} \leq c_1 h^{k-1} |\psi|_{H^{k+1}_\Omega}$$

and since $\psi_h - \mathcal{I}^h\psi$ belongs to $\mathcal{W}^h$ we can apply the inverse estimate (2.12) to yield

$$\|\psi_h - \mathcal{I}^h\psi\|_{H^2_\Omega} \leq c_2 h^{-2} \|\psi_h - \mathcal{I}^h\psi\|_{L^2_\Omega},$$

whereby (4.33) becomes

$$\begin{aligned}
\|\widetilde{e}\|_{H^2_\Omega} &\leq c_1 h^{k-1} |\psi|_{H^{k+1}_\Omega} + c_2 h^{-2} \|\psi_h - \mathcal{I}^h\psi\|_{L^2_\Omega} \\
&= c_1 h^{k-1} |\psi|_{H^{k+1}_\Omega} + c_2 h^{-2} \|\psi_h - \psi + \psi - \mathcal{I}^h\psi\|_{L^2_\Omega} \\
&\leq c_1 h^{k-1} |\psi|_{H^{k+1}_\Omega} + c_2 h^{-2} (\|\widetilde{e}\|_{L^2_\Omega} + \|\psi - \mathcal{I}^h\psi\|_{L^2_\Omega}).
\end{aligned}$$

Applying (2.10) to the last norm and using (4.30), we get

$$\begin{aligned}
\|\widetilde{e}\|_{H^2_\Omega} &\leq c_1 h^{k-1} |\psi|_{H^{k+1}_\Omega} + c_2 h^{-2} (\|\widetilde{e}\|_{L^2_\Omega} + c_1 h^{k-1} |\psi|_{H^{k+1}_\Omega}) \\
&\leq c_1 h^{k-1} |\psi|_{H^{k+1}_\Omega} + c_2 h^{-2} (\mathcal{C}_1 h^{k+1} |\psi|_{H^{k+1}(\Omega)} + c_1 h^{k+1} |\psi|_{H^{k+1}_\Omega}),
\end{aligned}$$

which is the estimate (4.32) with $c_4 = c_1 + c_2\mathcal{C}_1 + c_1 c_2$. □

5. Numerical results

In this section, numerical results for several benchmark problems are studied to explore whether the optimal error estimates derived in the previous sections apply. The linear Stommel–Munk model is a fourth-order PDE. Hence, a standard finite-element approximation requires the solution space $\mathcal{W}^h$ to be globally H^2 conforming — that is, C^1-continuous basis functions with continuity of the stream-function field and of its first derivatives.

For cubic B-splines, the order of the polynomial is $k = 3$. Hence, the optimal convergence rates are quartic, cubic, and quadratic for the L^2-norm, the H^1-norm, and the H^2-norm (only for the Stommel–Munk model) of the error based on error estimates in Sections 3 and 4, respectively. Kim et al. [29] obtained the optimal rates of convergence on several benchmark problems without the error estimates. The Nitsche-type variational formulations (3.6) and (4.6) involve stabilization parameters which influence both convergence rates and the numerical accuracy. Kim et al. [29] evaluated these parameters by solving a local eigenvalue problem on the Dirichlet boundary. We choose these stabilization parameters based on the analyses (3.16) for the Stommel model and (4.14) for the Stommel–Munk model. Unless

otherwise indicated, the forcing term F for each test example is chosen to match that given by the corresponding closed-form solution.

We present some numerical tests for benchmark problems on rectangular region and on the same region with an embedded circular island. The results on the embedded geometries are obtained using a technique similar to those introduced by Dréau et al. [14], Jiang et al. [23], and Ruess et al. [38]. Although our error analysis does not cover explicitly these methods, it can be easily generalised, and our simulations show optimal convergence rates also in these cases.

For embedded geometries, the boundary of the domain is described implicitly by level set functions. This non-boundary-fitted approach makes it possible to generate simple meshing of potentially very complex domains, for which an exact geometrical representation expressed as in equation (2.5) may not be available. In such cases, the imposition of the boundary condition we present in this paper carries over in a natural way, provided that it is possible to integrate accurately the weak terms along the embedded boundary. A simple way to increase the level of accuracy in the geometric representation of the boundary is to use hierarchical sub-meshes in a vicinity of the boundary only for the geometrical representation, while maintaining the same B-splines spaces defined in (2.15) and (2.16) for the approximation spaces. This approach improves the geometrical representation of the boundary while maintaining the same coarse mesh for the B-splines basis and allows the analysis of the previous sections to carry over in a straight forward manner.

5.1. **The Stommel model.** In this section, we verify the error estimates of (3.33) and (3.34) for the Stommel model. We take the stabilization parameter $\alpha = 1/2p + \epsilon_{\mathrm{s}} C/p^2 h$ from (3.16) with $p = 1/2$ and $C = 10^2$.

We first begin by performing a convergence study on a rectangular region $\Omega = [0,3] \times [0,1]$ using two test problems with the closed-form solutions

$$\psi(x,y) = \sin^2(\pi x/3)\sin^2(\pi y) \quad \text{in } \Omega = [0,3] \times [0,1] \tag{5.1}$$

and

$$\begin{aligned}\psi(x,y) = \frac{\sin(\pi y)}{\pi(1+4\pi^2\epsilon_{\mathrm{s}}^2)}\{&2\pi\epsilon_{\mathrm{s}}\sin(\pi x) \\ &+ \cos(\pi x) + [(1+e^{R_2})e^{R_1 x} - (1+e^{R_1})e^{R_2 x}]/(e^{R_1} - e^{R_2})\}.\end{aligned} \tag{5.2}$$

In (5.2), R_1 and R_2 are given by

$$R_1 = \frac{-1+\sqrt{1+4\pi^2\epsilon_{\mathrm{s}}^2}}{2\epsilon_{\mathrm{s}}} \quad \text{and} \quad R_2 = \frac{-1-\sqrt{1+4\pi^2\epsilon_{\mathrm{s}}^2}}{2\epsilon_{\mathrm{s}}}.$$

Figure 1 displays the streamlines from the numerical solutions for the two test problems. While the test problem (5.2) (Figure 1(b)) displays a thin boundary layer in the vicinity of $x = 0$ corresponding to a western boundary layer, the test problem (5.1) (Figure 1(a)) does not display a boundary layer. These test problems were commonly used to test finite-element algorithms for large-scale ocean circulation problems (Myers and Weaver [34], Foster et al. [19]). To allow comparisons with results from, we choose the Stommel number $\epsilon_{\mathrm{s}} = 0.05$.

Figure 2 displays the convergence rates for the test problem (5.1) without a boundary layer and the test problem (5.2) with a boundary layer. Plots are provided for the convergence rates in two error norms: the L^2-norm and the H^1-norm. For cubic B-splines, the optimal rates are quartic and cubic in the L^2-norm and H^1-norm of the error, respectively, as found in Section 3. As shown in Figure 2(a),

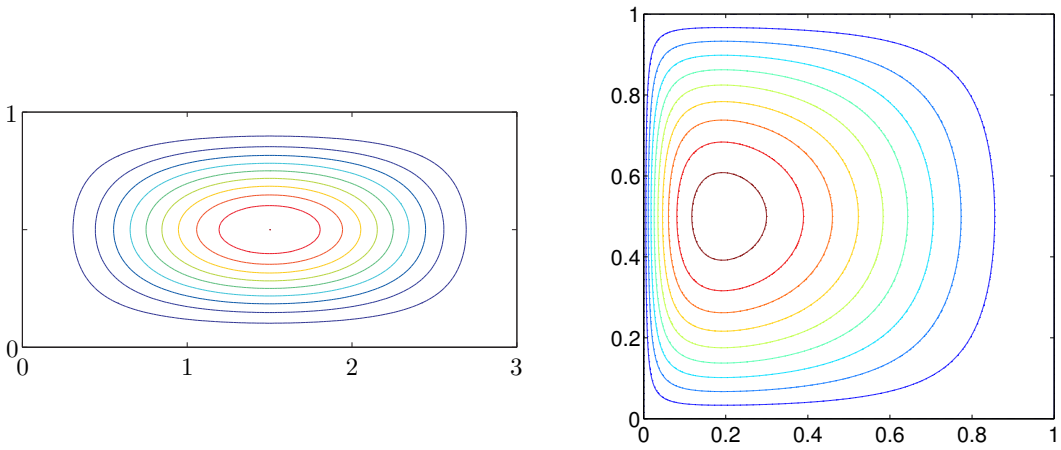

(a) (b)

FIGURE 1. The Stommel model: Streamlines of the approximation to the solution on a mesh size of $h = 1/64$.

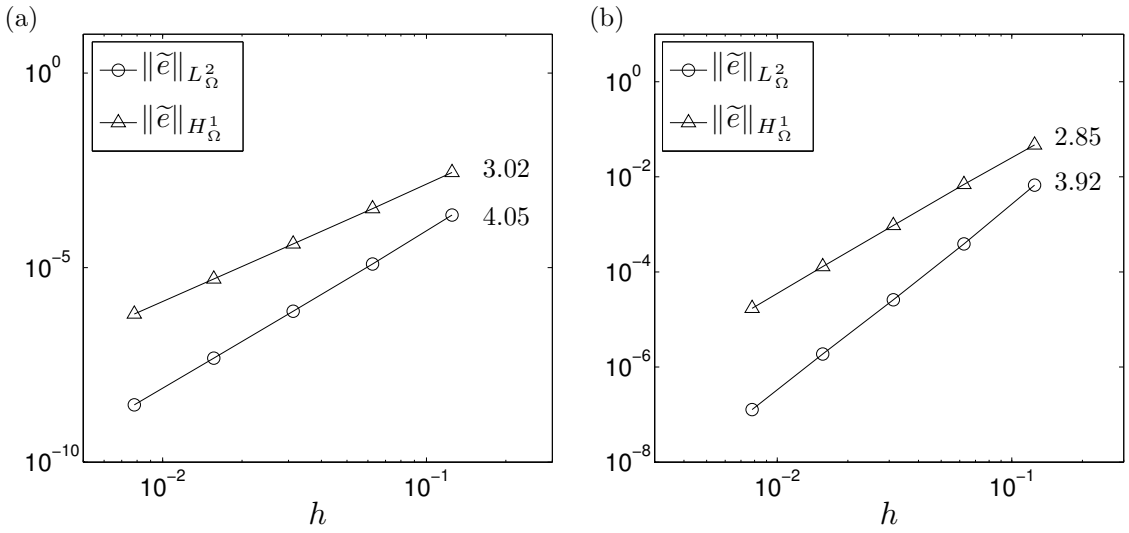

FIGURE 2. The Stommel model: Convergence rates in the L^2-norm and the H^1-norm for the test problems: (a) (5.1) without a boundary layer and (b) (5.2) with a western boundary layer.

we observe optimal convergence rates in both norms for the test problem (5.1). Figure 2(b) displays the rates of convergence for the test problem (5.2). In contrast to the test problem (5.1), slightly lower convergence rates are observed in both norms. We attribute this to the presence of the western boundary layer, as do Foster et al. [19].

Our second example is a convergence study on a square region $\Omega = [0,1] \times [0,1]$ with an embedded circular island of radius 0.3 using the closed-form solution

$$\psi(x,y) = \sin^2((x+1)/2\pi)\sin^2((y+1)/2\pi)\sin^2(x^2+y^2-0.3^2). \tag{5.3}$$

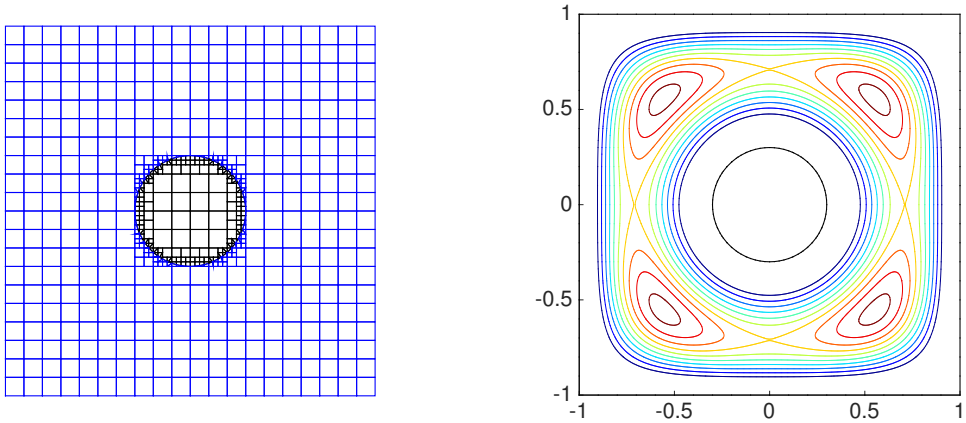

(a) (b)

FIGURE 3. The Stommel model: (a) The square region $\Omega = [0, 1] \times [0, 1]$ with a circular central island of radius 0.3 embedded in a finite-element mesh. (b) Streamlines of the approximation to the solution on a mesh size of $h = 0.1$.

Figure 3(a) shows a finite-element mesh model with the mesh size $h = 0.1$. The circular inner boundary is implicitly represented by a level set function, and a hierarchical sub-mesh in the vicinity of the boundary is used to increase the accuracy of the geometrical representation.

Figure 3(b) shows the streamlines of the numerical solution obtained using the finite-element mesh shown in Figure 3(a). Figure 4 shows the convergence rate in the L^2- and H^1-norms. The rates of convergence for both norms are optimal. These results verify optimal error estimates in the L^2-norm (3.33) and the H^1-norm (3.34) provided in Section 3 on both rectangular and embedded geometries.

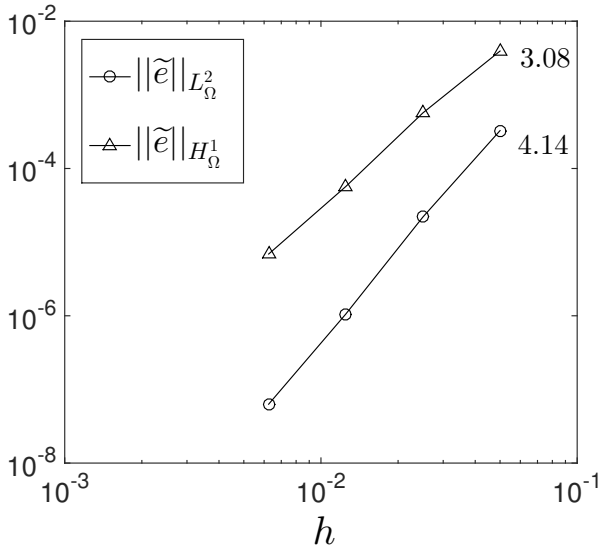

FIGURE 4. The Stommel model: Convergence rates in the L^2-norm and the H^1-norm for the test problem (5.3).

5.2. **The Stommel–Munk model.** In this section, we verify the error estimates of (4.30), (4.31), and (4.32) for the Stommel–Munk model. Numerical studies are first performed on the rectangular region $\Omega = [, 3] \times [0, 1]$ for test problems with the exact solutions (5.1) and

$$\psi(x, y) = [(1 - x/3)(1 - e^{-20x}) \sin(\pi y)]^2 \quad \text{in } \Omega = [0, 3] \times [0, 1]. \tag{5.4}$$

These solutions have previously been used to test a finite-element algorithm for large-scale ocean circulation problems (Cascon et al. [8], Foster et al. [19]).

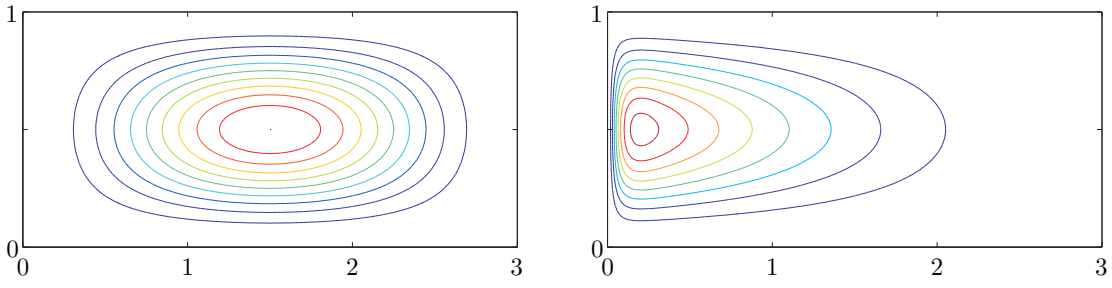

(a) (b)

FIGURE 5. The Stommel–Munk model: Plots of the numerical solutions for the test problems with exact solutions of (a) (5.1) without a boundary layer and (b) (5.4) with a western boundary layer.

Figure 5 displays the plots of the numerical solutions for the two test problems. As shown in Figure 5(b), the test problem (5.4) displays a thin boundary layer in the vicinity of $x = 0$ corresponding to a western boundary layer. On the other hand, the test problem (5.1) shown in Figure 5(a) does not display a boundary layer. Our

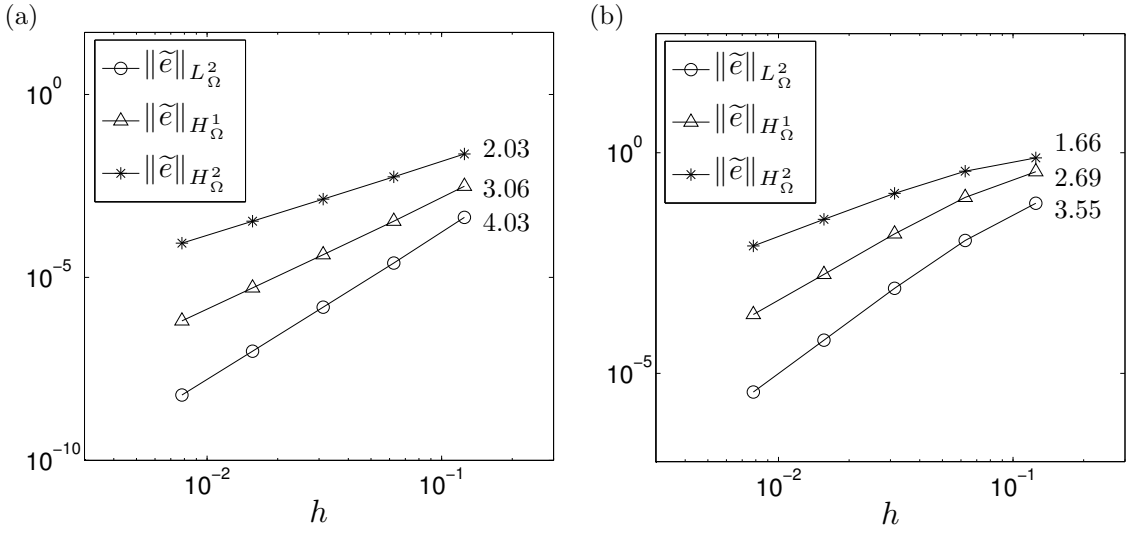

FIGURE 6. The Stommel–Munk model: Convergence rates in the L^2-norm, the H^1-norm, and the H^2-norm for the test problems: (a) (5.1) without any boundary layer and (b) (5.2) with a western boundary layer.

computational setting is made identical to that used by Cascon et al. [8] and Foster et al. [19] by taking the Munk number $\epsilon_{\rm m} = 6 \times 10^{-5}$ and the Stommel number $\epsilon_{\rm s} = 0.05$. We also take $\alpha_1 = 1/2r + \epsilon_{\rm s} C_1/r^2 h$ and $\alpha_2 = 4\epsilon_{\rm m} C_2/r^2 h$ from (4.14) with $r = 1/2$, $C_1 = 10^3$, and $C_2 = 10^2$.

Figure 6 displays the convergence rates for both test problems (5.1) and (5.4). Optimal convergence rates in all norms for the test problem (5.1) without any boundary layer are observed. On the other hand, slightly lower convergence rates in all norms are observed for the test problem (5.4) due most likely to the presence of the western boundary layer, as Foster et al. [19] hypothesize.

We next study the performance of the proposed algorithm for the Stommel–Munk model on embedded geometries. Our study is conducted on a rectangular shaped domain with a circular island using the exact solution (5.3), as in our study of the Stommel model. We use the same finite-element mesh in Figure 3(a). To avoid repetition, the streamlines of the numerical solutions are no longer displayed. However, the streamlines are indistinguishable from those of Figure 3(b).

Similar to the Stommel model, in Figure 7, we display the convergence rates in the L^2-, H^1-, and H^2-norms of the error. The rates of convergence of these norms are optimal. These results verify the analyses of (4.30), (4.31), and (4.32) for the Stommel–Munk model on both rectangular and embedded geometries.

6. Conclusions

In this paper, we studied error estimates for B-spline based Nitsche-type variational formulations of the Stommel and Stommel–Munk models for the large scale wind-driven ocean circulation simulation. These formulations were introduced by Kim et al. [29] for non-interpolatory basis functions. In contrast to the standard conforming finite-element formulations, these formulations involve additional terms to weakly enforce Dirichlet boundary conditions along with stabilization terms. Our

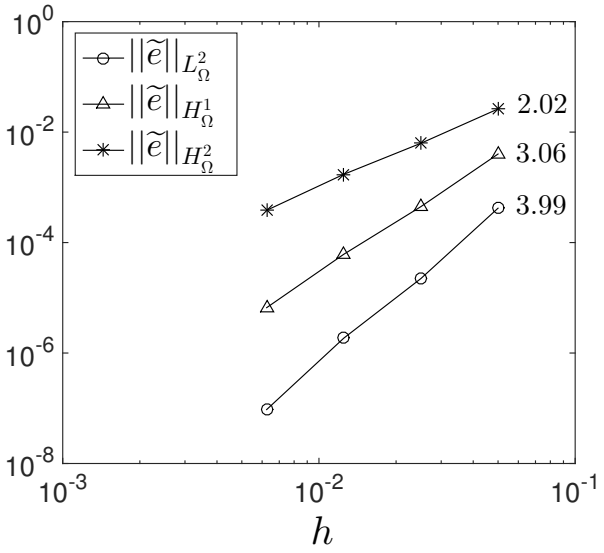

FIGURE 7. The Stommel–Munk model: Convergence rates in the L^2-, H^1-, and H^2-norms for the test problem (5.3).

analysis established the optimal convergence rates of $k+1$ in the L^2-norm, k in the H^1-norm, and $k-1$ in the H^2-norm for the kth-order non-interpolatory polynomial basis functions. Such variational formulations involve stabilization parameters which influence both convergence rates and the numerical accuracy. Kim et al. [29], introduced such parameters without proving their error properties and estimated them by solving local eigenvalue problems on the Dirichlet boundaries. The estimates obtained in this paper establish the robustness of these formulations and allow the selection of the stabilisation parameters without solving any additional problem. Several numerical examples using cubic B-splines demonstrated the error analyses for both models on a rectangular domain and a square domain with an embedded circular island.

For a rectangular region without embedded domains, optimal rates of convergence were observed for all test problems, with a slight loss of performance in the example with a thin western boundary layer. For a square region containing an embedded circular island, optimal rates of convergence were obtained for both Stommel and Stommel–Munk models, indicating that embedded boundaries can be used in conjunction with the proposed method to capture arbitrarily shaped coastal boundaries with good accuracy. This is an important consequence of the weak formulation.

In the future, we plan to extend our error estimates for the Nitsche-type variational formulation of the nonlinear SQGE. Moreover we hope to extend our finite-element discretization using hierarchical B-splines or T-splines and to add *a posteriori* error estimates to capture more efficiently and accurately with thin boundary layers. Finally, we intend to extend this study to the time-dependent QGE and the two-layer QGE.

Acknowledgements

The work has been partially supported by (N.R.) ERC-2010-AdG no. 267802 Analysis of Multiscale Systems Driven by Functionals, and by (L.H.) project OpenViewSHIP, "Sviluppo di un ecosistema computazionale per la progettazione idrodinamica del sistema elica-carena", supported by Regione FVG - PAR FSC 2007-2013, Fondo per lo Sviluppo e la Coesione and by the project "TRIM – Tecnologia e Ricerca Industriale per la Mobilità Marina", CTN01-00176-163601, supported by MIUR, the Italian Ministry of Instruction, University and Research.

References

[1] D. N. Arnold. An interior penalty finite element method with discontinuous elements. *SIAM Journal on Numerical Analysis*, 19(4):742–760, 1982.

[2] Y. Bazilevs and T. J. R. Hughes. Weak imposition of Dirichlet boundary conditions in fluid mechanics. *Computers & Fluids*, 36(1):12–26, 2007.

[3] Y. Bazilevs, L. Beirão Da Veiga, J. A. Cottrell, T. J. R. Hughes, and G. Sangalli. Isogeometric analysis: Approximation, stability and error estimates for h-refined meshes. *Mathematical Models and Methods in Applied Sciences*, 16 (07):1031–1090, July 2006. ISSN 0218-2025.

[4] Y. Bazilevs, C. Michler, V. M. Calo, and T. J. R. Hughes. Isogeometric variational multiscale modeling of wall-bounded turbulent flows with weakly enforced boundary conditions on unstretched meshes. *Computer Methods in Applied Mechanics and Engineering*, 199(13):780–790, 2010.

[5] D. Boffi, L. Gastaldi, L. Heltai, and C. S. Peskin. On the hyper-elastic formulation of the immersed boundary method. *Computer Methods in Applied Mechanics and Engineering*, 197(25-28):2210–2231, 2008.

[6] J. H. Bramble, T. Dupont, and V. Thomée. Projection methods for Dirichlet's problem in approximating polygonal domains with boundary-value corrections. *Mathematics of Computation*, 26(120):869–879, 1972.

[7] S. Brenner and R. Scott. *The Mathematical Theory of Finite Element Methods*. Springer Science & Business Media, 2007. ISBN 9780387759333.

[8] J. M. Cascon, G. C. Garcia, and R. Rodriguez. A priori and a posteriori error analysis for a large-scale ocean circulation finite element model. *Computer Methods in Applied Mechanics and Engineering*, 192(51):5305–5327, 2003.

[9] P. Ciarlet. *The Finite Element Method for Elliptic Problems*. SIAM, 2002. ISBN 0898715148.

[10] J. A. Cottrell, T. J. R. Hughes, and Y. Bazilevs. *Isogeometric analysis: Toward integration of CAD and FEA*. John Wiley & Sons Inc, 2009.

[11] B. Cushman-Roisin and J. Beckers. *Introduction to Geophysical Fluid Dynamics: Physical and Numerical Aspects*. Academic Press, 2011.

[12] L. B. da Veiga, A. Buffa, J. Rivas, and G. Sangalli. Some estimates for h–p–k-refinement in isogeometric analysis. *Numerische Mathematik*, 118(2):271–305, 2011.

[13] J. Dolbow and I. Harari. An efficient finite element method for embedded interface problems. *International Journal for Numerical Methods in Engineering*, 78(2):229–252, 2009.

[14] K. Dréau, N. Chevaugeon, and N. Moës. Studied X-FEM enrichment to handle material interfaces with higher order finite element. *Computer Methods in Applied Mechanics and Engineering*, 199(29–32):1922 – 1936, 2010. ISSN 0045-7825.

[15] A. Embar, J. Dolbow, and I. Harari. Imposing Dirichlet boundary conditions with Nitsche's method and spline-based finite elements. *International Journal for Numerical Methods in Engineering*, 83(7):877–898, 2010.

[16] G. Engel, K. Garikipati, T. Hughes, M. Larson, L. Mazzei, and R. Taylor. Continuous/discontinuous finite element approximations of fourth-order elliptic problems in structural and continuum mechanics with applications to thin beams and plates, and strain gradient elasticity. *Computer Methods in Applied Mechanics and Engineering*, 191(34):3669–3750, July 2002. ISSN 00457825.

[17] S. Fernández-Méndez and A. Huerta. Imposing essential boundary conditions in mesh-free methods. *Computer Methods in Applied Mechanics and Engineering*, 193(12):1257–1275, 2004.

[18] G. J. Fix. Finite element models for ocean circulation problems. *SIAM Journal on Applied Mathematics*, 29(3):371–387, 1975.

[19] E. Foster, T. Iliescu, and Z. Wang. A finite element discretization of the streamfunction formulation of the stationary quasi-geostrophic equations of the ocean. *Computer Methods in Applied Mechanics and Engineering*, 2013.

[20] A. Hansbo and P. Hansbo. An unfitted finite element method, based on Nitsche's method, for elliptic interface problems. *Computer methods in applied mechanics and engineering*, 191(47-48):5537–5552, 2002. ISSN 0045-7825.

[21] L. Heltai, M. Arroyo, and A. DeSimone. Nonsingular isogeometric boundary element method for stokes flows in 3d. *Computer Methods in Applied Mechanics and Engineering*, 268:514–539, 2014.

[22] T. Hughes, J. Cottrell, and Y. Bazilevs. Isogeometric analysis: CAD, finite elements, NURBS, exact geometry and mesh refinement. *Computer Methods in Applied Mechanics and Engineering*, 194(39-41), 2005.

[23] W. Jiang, C. Annavarapu, J. E. Dolbow, and I. Harari. A robust Nitsche's formulation for interface problems with spline-based finite elements. *International Journal for Numerical Methods in Engineering*, 2015. ISSN 1097-0207.

[24] D. Kamensky, M.-C. Hsu, D. Schillinger, J. A. Evans, A. Aggarwal, Y. Bazilevs, M. S. Sacks, and T. J. Hughes. An immersogeometric variational framework for fluid–structure interaction: Application to bioprosthetic heart valves. *Computer methods in applied mechanics and engineering*, 284:1005–1053, 2015.

[25] T.-Y. Kim and J. E. Dolbow. An edge-bubble stabilized finite element method for fourth-order parabolic problems. *Finite Elements in Analysis and Design*, 45(8):485–494, 2009.

[26] T.-Y. Kim, J. Dolbow, and E. Fried. A numerical method for a second-gradient theory of incompressible fluid flow. *Journal of Computational Physics*, 223(2): 551–570, 2007.

[27] T.-Y. Kim, J. E. Dolbow, and E. Fried. Numerical study of the grain-size dependent Young's modulus and Poisson's ratio of bulk nanocrystalline materials. *International Journal of Solids and Structures*, 49(26):3942–3952, 2012.

[28] T.-Y. Kim, E. Puntel, and E. Fried. Numerical study of the wrinkling of a stretched thin sheet. *International Journal of Solids and Structures*, 49(5): 771–782, 2012.

[29] T.-Y. Kim, T. Iliescu, and E. Fried. B-spline based finite-element method for the stationary quasi-geostrophic equations of the ocean. *Computer Methods in Applied Mechanics and Engineering*, 286:168–191, 2015.

[30] A. Majda. *Introduction to PDEs and Waves for the Atmosphere and Ocean*, volume 9. American Mathematical Soc., 2003.

[31] A. Majda and X. Wang. *Nonlinear Dynamics and Statistical Theories for Basic Geophysical Flows*. Cambridge University Press, 2006.

[32] A. Manzoni, F. Salmoiraghi, and L. Heltai. Reduced Basis Isogeometric Methods (RB-IGA) for the real-time simulation of potential flows about parametrized NACA airfoils. *Computer Methods in Applied Mechanics and Engineering*, 284:1147–1180, 2015.

[33] J. C. McWilliams. *Fundamentals of Geophysical Fluid Dynamics*. Cambridge University Press, 2006.

[34] P. G. Myers and A. J. Weaver. A diagnostic barotropic finite-element ocean circulation model. *Journal of Atmospheric and Oceanic Technology*, 12(3): 511–526, 1995.

[35] J. Nitsche. Uber ein variationsprinzip zur lösung von dirichlet-problemen bei verwendung von teilräumen, die keinen randbedingungen unterworfen sind. In *Abhandlungen aus dem mathematischen Seminar der Universität Hamburg*, volume 36, pages 9–15. Springer, 1971.

[36] J. Pedlosky. *Geophysical Fluid Dynamics*. Springer Science & Business Media, 2013.

[37] L. Piegl and W. Tiller. *The NURBS book (2nd ed.)*. Springer–Verlag New York, Inc., New York, NY, USA, 1997.

[38] M. Ruess, D. Schillinger, Y. Bazilevs, V. Varduhn, and E. Rank. Weakly enforced essential boundary conditions for NURBS-embedded and trimmed NURBS geometries on the basis of the finite cell method. *International Journal for Numerical Methods in Engineering*, 95(10):811–846, 2013. ISSN 1097-0207.

[39] G. Vallis. *Atmospheric and Oceanic Fluid Dynamics: Fundamentals and Large-scale Circulation*. Cambridge University Press, 2006.